

## Article

# Projecting Bioclimatic Change over the South-Eastern European Agricultural and Natural Areas via Ultrahigh-Resolution Analysis of the de Martonne Index

Ioannis Charalampopoulos \* , Fotoula Droulia and Ioannis X. Tsiros

Laboratory of General and Agricultural Meteorology, Department of Crop Science, Agricultural University of Athens, 11855 Athens, Greece; fdroulia@aua.gr (F.D.); itsiros@aua.gr (I.X.T.)

\* Correspondence: icharalamp@aua.gr; Tel.: +30-210-5294234

**Abstract:** The changing climate is closely related to changes in the bioclimate. This research deals with the present bioclimate and its projected evolution over the entirety of the natural and agricultural lands of south-eastern Europe and individual countries (Bulgaria, Greece, Kosovo, N. Macedonia, Romania, and Serbia). For this purpose, an ultrahigh spatial resolution of the de Martonne bioclimatic index pattern was elaborated and analysed for the first time. The survey is performed over the reference period (1981–2010) and future time frames (2011–2040; 2041–2070; 2071–2100) under SSP370 and SSP585 emission scenarios. On a territorial level, both natural and agricultural areas appear as highly impacted by the future changes of bioclimate; the highest xerothermic trend is expected to influence the latter areas, mostly in 2071–2100 and under the higher emission scenario. The natural areas will face an expansion in the semidry class from 0.9% (of the total area) during the reference period to 5.6% during 2071–2100 under the RCP8.5 scenario as the dominant extremely humid class falls from 53.5% to 32.9% for the same periods and scenario. On the other hand, agricultural areas will face a more intense xerothermic alteration going from 4.9% to 17.7% for the semidry class and from 41.1% to 23.5% for the dominant very humid class for the same periods and scenario. This study presents the spatial statistics per country for the selected scenarios and periods to provide information for stakeholders. This study's results highlight the necessity for intensifying adaptation plans and actions aiming at the feasibility of agricultural practices and the conservation of natural areas.

**Keywords:** climate change; bioclimate change; bioclimate classification; de Martonne index; Bulgaria; Greece; Kosovo; N. Macedonia; Romania; Serbia



**Citation:** Charalampopoulos, I.; Droulia, F.; Tsiros, I.X. Projecting Bioclimatic Change over the South-Eastern European Agricultural and Natural Areas via Ultrahigh-Resolution Analysis of the de Martonne Index. *Atmosphere* **2023**, *14*, 858. <https://doi.org/10.3390/atmos14050858>

Academic Editor: Ilias Kavouras

Received: 18 April 2023

Revised: 5 May 2023

Accepted: 9 May 2023

Published: 11 May 2023



**Copyright:** © 2023 by the authors. Licensee MDPI, Basel, Switzerland. This article is an open access article distributed under the terms and conditions of the Creative Commons Attribution (CC BY) license (<https://creativecommons.org/licenses/by/4.0/>).

## 1. Introduction

The international scientific community's focus on the developing phenomenon of climate change (CC) is well established in this context, and research also focuses on bioclimate change by considering its impacts on living organisms, landscapes, land use, exploitation of resources, ecosystem services and management strategies [1–6].

The part of south-eastern Europe (PSEEu) comprising six countries (in alphabetical order: Bulgaria—BG; Greece—GR; Kosovo—XK; N. Macedonia—MK; Romania—RO; Serbia—RS) appear as a future hotspot in the CC context [7]. Projections depict the constant warming leading to an approximate increase of 0.9 °C in annual mean temperature by 2070 and 7 °C by 2100, during the summer. This, along with projections of the decreasing precipitation amounts by nearly 300–400 mm in the east of the region and northern Greece by 2070, will lead to the region's degree of aridity [8]. In addition, according to some studies, CC is closely associated with extreme weather events' intensity and frequency increase [7–9], and there is published research indicating the high uncertainty of the impact of climate change on extreme weather events [9,10]. Moreover, this part of the European continent is in a transitional climatic zone that will face abrupt changes in the major atmospheric parameters affecting ecosystems and crops due to climate change [11–13]. The

above characteristics of the area together with its known biodiversity importance necessitate the argument for a thorough study of its present and future bioclimatic situation.

Projections on the climate evolution of PSEEU and the prevailing greater region's xerothermic regime highlight its susceptibility to CC with impacts on natural vegetation and rural areas [14,15]. The impacts of CC on natural systems commonly refer to the increased vulnerability of forest species owing to intensified aridisation and higher fire risks [16,17], tree growth limitation and defoliation, forest withering and dieback [18–20], degradation of forest and grassland ecosystems [21], biodiversity decline [22] and the more intensified risk of biological invasions (e.g., of alien plant species and invasive insects) [23,24]. The underlying role of the alternating environment involves crucial impacts on the agricultural sector of the PSEEU, mainly referring to increased plant stress due to water scarcity [25], recurrent plant injuries due to elevated heat stress [11], insufficient recharge of ground and surface water [26], increased plant evapotranspiration [27], increased yield variability [28], agricultural production's quality and quantity decline [29–31], and crops' expansion to more climatically suitable areas for their development and production [7,11,32,33].

Climate change and its impacts on vegetation and vegetation types' distribution are better achieved, in bioclimatic terms, using the values resulting from mathematical formulas of climatic parameters corresponding to bioclimatic indices [34,35]. The wide recognition of the bioclimatic indices is well demonstrated by their large-scale applications in agriculture science, bioclimatology and climatology [36–39].

The de Martonne index (IDM) is a key bioclimatic index used for the evaluation of a specific area's climatic level of dryness, which is categorised into seven (7) classes, from "dry" to "extremely humid", by the correlation of the air temperature and precipitation climatic parameters [8]. This index has widespread application due to its accuracy and effectiveness for the reliable classification of the climate's dryness degree [40], demonstrated by its frequent use in various studies (e.g., climatological, bioclimatic, hydrogeological and agricultural) [40–43]. IDM is widely used by the ecology and agriculture research community because it is an easy-to-calculate index with easy-to-obtain atmospheric parameters as input. Moreover, this index is very useful for environmental assessment reports.

In the Balkan Peninsula, Baltas [44] described the spatial pattern of aridity in northern Greece from 1965 to 1995 and denoted its variability with IDM values corresponding to a characterisation range from semidry to very humid conditions. For the same period, Baltas [44] also illustrated the bioclimatic footprint for the entire country (Greece), in which the values of IDM covered nearly the whole range of the climate classes, from dry to very humid. Mavrakis et al. [45], who investigated the long-term climate variations in the traditional agroforest system of Thriasio Plain (northwest of Athens, Greece), concluded a moderate trend towards a warmer and drier climate between 1958 and 2011. Beloiu et al. [46] highlighted the transition of the bioclimate from very humid to humid conditions over the 1979–2013 period in Crete Island (southern Greece). Based on a long-term (1990–2019) time series, Sidiropoulou et al. [47] classified Mt Vermio (north Greece) and Mt Zireia (south Greece) as moderately humid and humid, respectively. Mattas et al. [48] calculated the IDM based on a 27-year (1980–2006) climatic data series and revealed the climate variation of the upper part of the agricultural area of the Gallikos river basin (northern Greece) from semiarid to humid. For the 1980 to 2001 period, Lappas et al. [49] demonstrated the bioclimatic classification of the water district of eastern–central Greece from arid to very humid.

Bačević et al. [50] reported no significant alterations in the bioclimate of Kosovo and Metohija (north-western Balkans) between 1965 and 1999. Hrnjak et al. [51] found no significant changes in the bioclimatic condition pattern in Vojvodina (northern Serbia) from 1949 to 2006. Similarly, Gavrilov et al. [52,53] concluded that, during approximately the same period (1949–2017), xerothermic trends remained unchanged in Vojvodina and SE Banat (Serbia). Moreover, no alterations in bioclimatic conditions were demonstrated by Radaković et al. [54] for central Serbia during the period 1949–2015. Moteva et al. [55] demonstrated highly variable annual IDM values over the Bulgarian territory and increased

aridity for the examined period (1971–2000). They also pointed out the usefulness of long-term IDM data for forecasting conditions for agricultural production.

Following estimations of the IDM for the 1961–2015 period, Vlăduț et al. [56] illustrated the predominance of semihumid conditions within southern Romania and northern Bulgaria and characterised the western and parts of the central sector of the Danube Valley as the most susceptible to bioclimatic warming and drying in both countries. Raev et al. [57] classified the current (1951–2000) bioclimate of Bulgaria and documented the future vulnerability of the country's forests owing to the projected aridisation for 2050 and 2070 under the RCP emissions scenarios.

According to Strat et al. [58], the results of the IDM suggest the dominance of a drier regime in the Sărăturile beach ridges plain (south-eastern part of the Danube Delta, Romania) during the 1990–2004 time period. Paltineanu et al. [59,60] demonstrated that, from 1900 to 2000, the driest conditions were characterised in the south-eastern areas of Romania and determined the index's relationship with irrigation water requirements of representative crops. In their survey on the spatial distribution of the IDM in the extra-Carpathian areas (southern, eastern and south-eastern parts of Romania) for the period 1961–2007, Croitoru et al. [61] also concluded that the areas most vulnerable to semi-aridity are the south-eastern regions of Romania. Vladut [62] classified the bioclimate of the Oltenia plain (south-western Romania) for 1984–2009 and documented tendencies towards a drier regime mainly in its southern, south-eastern and central parts. Similarly, Prăvălie [63] confirmed a pronounced alteration in the bioclimate over a longer five-decadal period (1961–2009) in southern Oltenia, where after 1980, the dominance of the semi-arid conditions is more evident. Long-term trends of the IDM in the study of Vlăduț and Licurici [64] resulted in the nonstatistically significant tendency of bioclimatic change over the entire Oltenia region between 1961 and 2015. Lungu et al. [65] highlighted Dobrudja's (south-western Romania) warmer and drier bioclimatic trend based on the computation of the index from the recorded climate data between 1965 and 2005. From calculations using the IDM, Prăvălie and Bandoc [66] also reported a general upward bioclimatic xerothermic trend in the same region (Dobrogea or Dobrudja) from 1961 to 2009, with the northern part being more affected by semiarid bioclimatic conditions. Following the computation of low IDM values for south Dobrudja during the years 1961–2000, Tiscovschi et al. [67] reported that aridity constitutes a major climatic risk, particularly for the eastern part of the investigated area, with negative impacts on agricultural productivity. The decrease in IDM values demonstrated by Vorovencii et al. [68] over the past decades (1984–2011) indicated the evolution of a xerothermic environment in the southwest of Romania, especially after 1980, when IDM values reflected a semiarid regime. The same classifications of south-western Romania's climate, owing to the downtrend in IDM for the 1990–2011 time period, were documented by Pravalie et al. [69], who reported the intensification of more arid bioclimatic conditions, resulting in forest biomass decline. Man et al. [70] revealed alternating wet and dry periods for Timisoara (western Romania) during the years 1980–2014, which were not considered indicative of aridisation or desertification for the years to come. Mihai et al. [71] calculated and analysed the IDM over provenance regions, subregions and ecological sectors (forest types) in Romania during the period 1951–2020. They highlighted the prevalence of more xerothermic conditions in the last three decades across provenance subregions. They also demonstrated that, during the vegetation season, the vast majority (86%) of ecological sectors were characterised by arid and semiarid bioclimatic conditions, indicative of major susceptibility of forests. To evaluate the climate effect on groundwater resources, Nistor [8] classified the bioclimate of the entire south-eastern European domain for the present (2011–2040) and future (2041–2070) periods under the RCP4.5 emissions scenario. Results for between the examined periods showed an increase in the spatial pattern of the Mediterranean and semidry classes, especially in the north, around the Pannonian basin, in south Romania and in central parts of Bulgaria. The extension of the semidry class was also depicted for the south-eastern parts of the examined region and the Aegean Islands. For almost the same geographical area, Cheval et al. [13] also reported significant

xerothermic trends under the A1B SRES IPCC scenario, given the expected replacement of the semi-humid category with the Mediterranean and even semidry categories, by 2050 in the eastern half of the Balkan Peninsula, especially along the Aegean coast.

The nature of the investigations based on the application of the IDM described above pinpoints the very limited scientific knowledge on the future evolution of the bioclimate on a subcontinental level. It has been demonstrated that most studies refer to past timeframes, mostly focus on the local scale and, to a much lesser extent, on the country level where, as very few studies of a sub-European geographical magnitude exist, the examined scenarios are limited (e.g., RCP4.5, AB1 SRES IPCC) and the adopted degree of spatial resolution is relatively low (1 km or 25 km).

Despite the known usefulness of this longitudinal index, there are (as far as we know) currently no high spatial resolution studies showing its evolution in the future under climate change conditions. Keeping in mind the relatively limited studies related to IDM applications and the importance of the preservation of cultivated and natural plant formations and their susceptibility to the changing bioclimate, the present study considers investigating the evolution of the bioclimate in the PSEEU, an area with particularly variable, extensive, and distinguished natural and agricultural areas. Changes in the spatiotemporal pattern of the IDM were investigated for the entire PSEEU and the natural and agricultural areas of the individual countries. The variability of the IDM was analysed over the reference period (Ref: 1981–2010) and three time periods (p1: 2011–2040; p2: 2041–2070; p3: 2071–2100), estimated at a high resolution of approximately 250 m under SSP370 (RCP7) and extreme SSP585 (RCP8.5) emissions scenarios. The short-term and long-term trends in bioclimatic change are discussed by considering the main differences between the present and future bioclimate regimes.

The originality of the current research lies in the ultrahigh-resolution computation (approximately 250 m) of the de Martonne index used to capture the present bioclimatic regime and its future evolution in a particularly extensive area represented by the entire PSEEU and its individual countries. The adoption of the RCP7 and RCP8.5 emission scenarios for future projections over the PSEEU is also documented for the first time.

## 2. Materials and Methods

### 2.1. Study Area

As shown by the landcover features in Figure 1, the natural landscape is almost evenly divided among mountains, hills, and plains in Romania. The country's agricultural areas are being developed in the Transylvanian Plain, enclosed within the great arc of the Carpathians (eastern–western Carpathians and Transylvanian Alps). Agricultural areas are also expanding in the eastern part of Romania (Moldavian Plain), in the southeast (Dobrujan Plateau), and the southern Plains (Danubian Plain, Wallachian Plain and the Oltenia Plain subregion).

Fertile agricultural plains are illustrated for northern landlocked Serbia (Pannonian Plain/Vojvodina region). At the same time, mountainous natural formations dominate the eastern (Serbian Carpathians), western (Zlatibor, Kopaonik Mountains) and southern parts of the country (Balkan Mountains), enclosing rural areas (valley of Morava). Mountainous natural areas surround the non-coastal Kosovo, the Kopaonik Mountains in the north, the Šarr (or Šar) Mountains in the southern and south-eastern borders, the Albanian Alps on the western edge of the country and the Goljak mountainous region in the east. These areas define the country's plains, characterised by agricultural exploitation (Metohija Basin and the Plain of Kosovo).

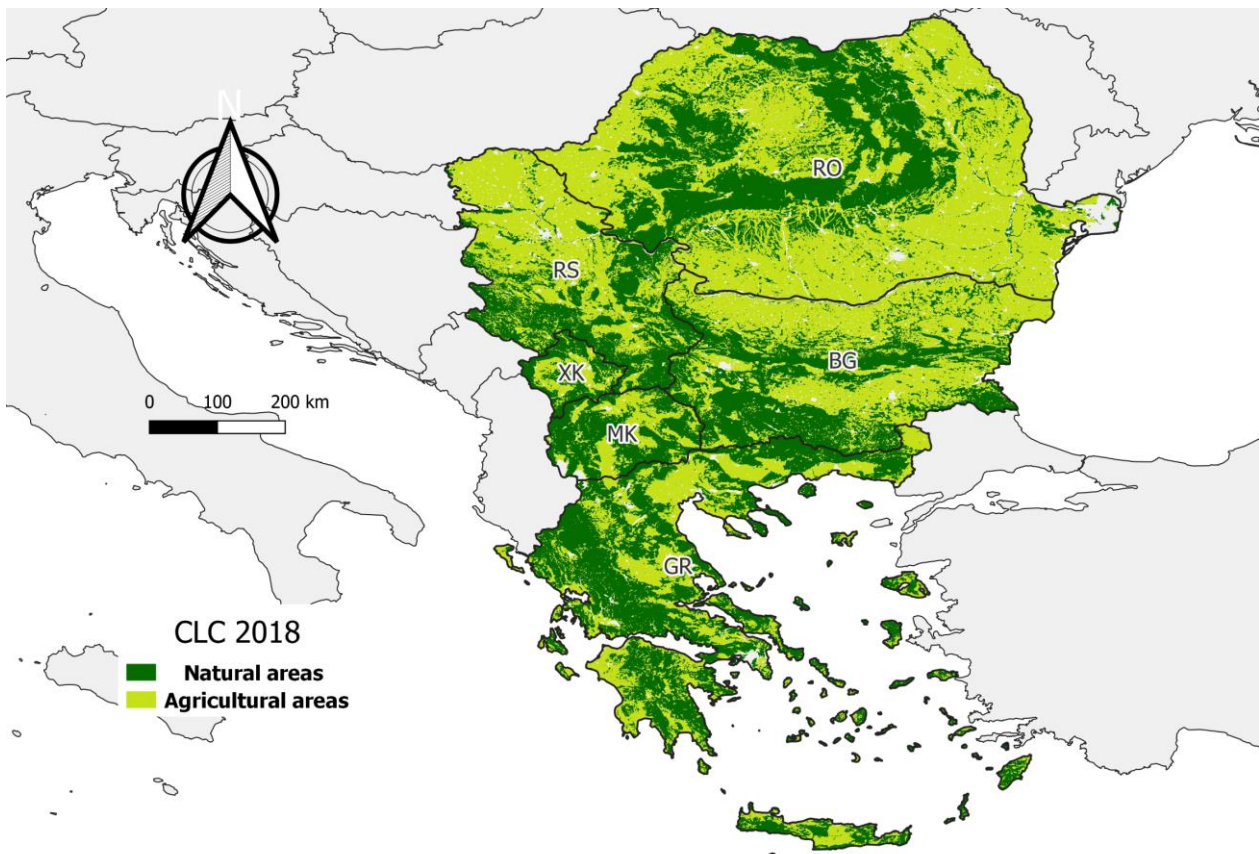


**Figure 1.** The generalised CORINE land cover 2018 (CLC 2018) illustrates the studied area's (territory's) natural and agricultural areas (BG = Bulgaria; GR = Greece; MK = North Macedonia; RO = Romania; RS = Serbia; XK = Kosovo).

Alternating bands of natural and agricultural areas extending from the east to the west appear for Bulgaria. From north to south, these bands consist of highly extensive rural areas (Danubian Plain), mountainous formations (Balkan Mountains or Stara Planina), fertile agricultural areas (Thracian Plain) and southern mountainous areas (Rhodope and Pirin Mountains). Dominating mountain ranges frame North Macedonia along its borders (Sharr, Osogovo, Malevenski and Nidze Mountains), defining its agricultural areas (e.g., the valley of the Vardar River or Vardar River Valley).

Natural areas occupy a significant part of mainland Greece, with the mountain formations present on the Greek–Bulgarian border (vastly forested Rhodope Mountains) or extending from the Greek–Albanian border to the Corinthian Gulf (Pindos Mountain range), continuing in the Peloponnese (Teygetos Mountain range) and appearing in Crete (White Mountains or Lefka Ori, Idi Mountain range and Dikti Mountains). These mountain ranges encompass highly productive agricultural plains and valleys across mainland Greece (e.g., Thessaloniki Plain, Thessaly Plain, plains of northern Peloponnese and central Crete). A high occupation of natural landscapes is also demonstrated for the majority of the Greek islands.

## 2.2. Data and Methods

Overall, the present survey's analytic process is constructed using the raster computation of the widely applied de Martonne bioclimatic index for four climatic time periods and under two greenhouse gas emissions scenarios in an ultra-high spatial resolution. The emissions scenarios include SSP370 and SSP585, which correspond, respectively, to RCP7 and RCP8.5 (Figure 2). The scenarios selected represent increased future greenhouse gas concentrations. SSP585 is the extreme scenario with the worst impacts, while SSP370 is used to

consider failure to take immediate and substantial action to reduce GHG emissions [72–78]. These scenarios have been chosen because, despite the efforts made so far at the global level, the reduction in greenhouse gas emissions has not reached the desired level. Moreover, the geopolitical situation since the start of the Russo–Ukrainian war further hinders joint action on climate change issues [79]. Although both scenarios involve high greenhouse gas emissions, they provide a basis for studying the impacts of climate change on agriculture and the natural environment [76,80–84]. The time frames involve the 1981–2010 reference period and the 2011–2040, 2041–2070 and 2071–2100 periods designated, respectively, as Ref, p1, p2 and p3.

### Data and Analysis Process

The extensive data employed in the present investigation are derived from the CHELSA repository [85,86], a widely recorded database commonly applied and used by researchers [87–90]. This database consists of multiple atmospheric indices and indicators accompanied by fundamental atmospheric parameters, including air temperature and precipitation in a spatial resolution of 30 arcsecs (~1 km). The CHELSA data corresponding to a period between 1979 and 2100 were compiled using reanalysis and bioclimate change projection approaches. The CHELSA atmospheric data downscaling to a resolution of less than 250 m (the typical resolution is 238.09 m for 0.0025 degrees) was performed using the regression process in spatialEco [91] together with the Tidyverse [92] and Terra [93] R packages. The air temperature data were downscaled by utilising altitude and latitude parameters along with the Euclidean distance from the shoreline, allowing for very high reliability when the precipitation data were resampled to the desired resolution using the bilinear method. Raster algebra methods have been used to perform IDM assessment for the periods regarding the adopted scenarios.

		Shared Socioeconomic Pathways (SSP) CMIP6					
		RCP Scenarios	SSP1 sustainability	SSP2 Middle of the road	SSP3 Regional rivalry	SSP4 Inequality	SSP5 Fossil fueled development
2100 forcing level (W.m <sup>-2</sup> )	8.5						SSP585
	7.0				SSP370		
	6.0					SSP460	
	4.5			SSP245			
	3.4					SSP434	SSP534
	2.6		SSP126				
	1.9		SSP119				

**Figure 2.** SSP–RCP scenario matrix illustrating their combination/association. Prepared with information from Rogelj et al. [94], Meinshausen et al. [95] and O’Neill et al. [96].

In the present study, the bioclimatic index of de Martonne (IDM) was calculated using an annual time step based on the application of the average precipitation (P) and temperature (T) values, as defined by the formula [97,98]:

$$IDM = \frac{P}{T + 10}$$

where:

- P is the annual precipitation (mm),
- T is the annual average air temperature (°C).

Higher IDM values specify humid bioclimatic conditions in contrast to dry bioclimatic conditions (or drier regimes) corresponding to lower values. The index can also be estimated at shorter timescales, e.g., seasonal and/or monthly. Bioclimate types associated with IDM values are shown in the classification scheme in Table 1. Seven bioclimate

characterizations from the arid or dry type to extremely humid type exists, also reflecting the respective levels of irrigation requirements.

**Table 1.** De Martonne index (IDM) categorisation, according to Passarella et al. [98].

IDM Values	Types of Bioclimates	Description
IDM < 10	Arid or dry	Needs continuous irrigation
10 ≤ IDM < 20	Semidry or semiarid	Needs irrigation
20 ≤ IDM < 24	Mediterranean	Needs supplementary irrigation
24 ≤ IDM < 28	Semi-humid	Needs supplementary irrigation
28 ≤ IDM < 35	Humid	Needs occasional irrigation
35 ≤ IDM ≤ 55	Very humid	Needs infrequent irrigation
IDM > 55	Extremely humid	Water self-sufficient

The commonly applied CORINE land cover (CLC) dataset [99] was used to distinguish the investigated territory’s agricultural and natural areas. For this purpose, the 2.1, 2.2, 2.3 and 2.4 CLC classes were considered agricultural areas and the 3.1, 3.2 and 3.3 classes as natural areas. The accuracy of the CLC exceeds 100 m, corresponding to relatively high thematic accuracy (≥85%) in the most recent year, 2018.

Exploiting the available landcover features and country border polygons for allowed the performance of spatial statistical analysis for the construction of comprehensive plots and maps utilized to detect bioclimatic qualitative and quantitative evolution across the PSEEU. The conducted analysis scheme is depicted in the flowchart of Figure 3.

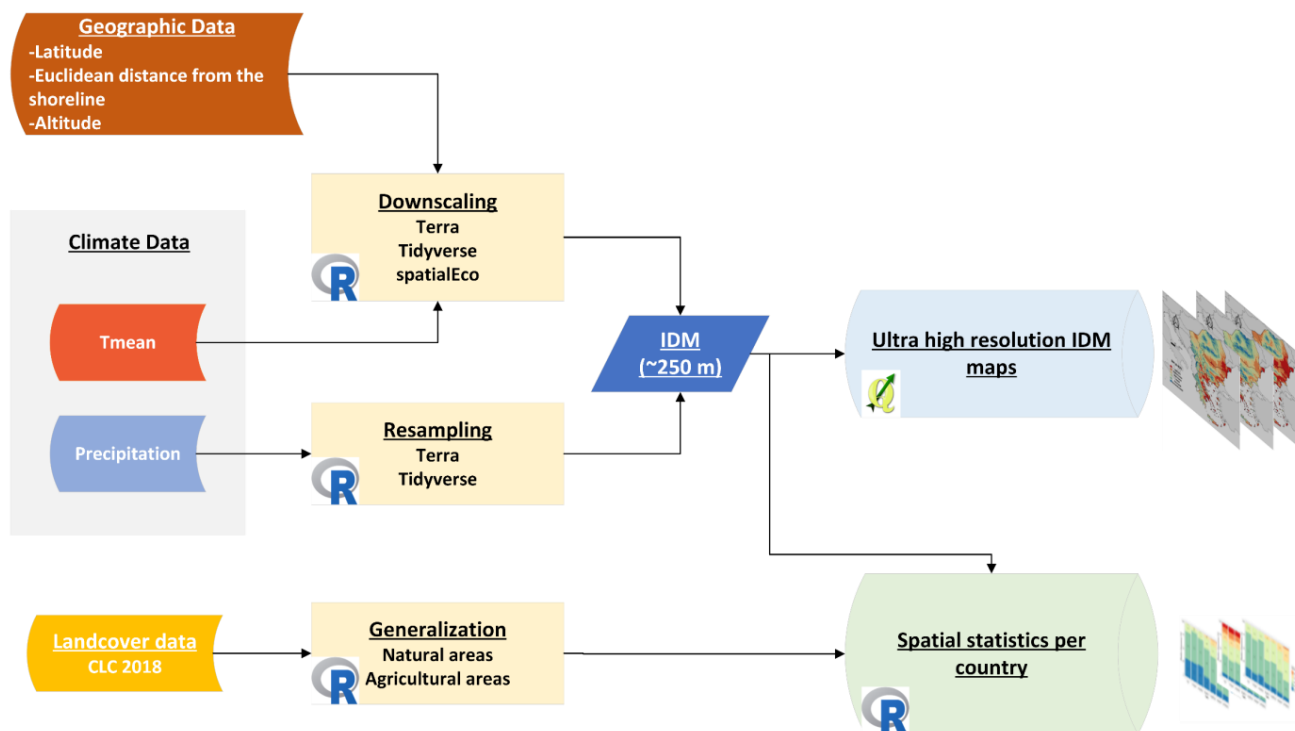


**Figure 3.** The performed analysis processes.

R language scripts were applied for overall data management, computations and analysis of the spatial and bioclimatic data. In detail, the application of the method used for this purpose requires the geographic data of latitude, altitude and Euclidean distance from the shoreline; the climate data derived from the CHELSA database; and the most recent CLC data derived from the Copernicus database as inputs. The downscaling process of the air temperature parameter (Tmean) was conducted using the spatialEco and Terra packages

for the handling of the raster data and Tidyverse for general data management. The critical factor for the resolution of the final downscaling is the resolution of the altitude raster. The precipitation data were resampled to the appropriate pixel size using the Terra package. Having the precipitation and the air temperature rasters in identical spatial characteristics, the IDM calculation was conducted. At the same time, the CLC dataset was reclassified to obtain thematic rasters containing the generalized natural and agricultural classes for use as masks to calculate spatial statistics. The bar plots were created using Tidyverse, and the mapping products were created using QGIS [100].

### 3. Results and Discussion

#### 3.1. Spatial Patterns of the de Martonne Index

According to the results (Figure 4) on the spatial distribution of de Martonne's categories over the reference period (1981–2000), the bioclimate of the PSEEU is distributed among six (6) classes: semidry, Mediterranean, semi-humid, humid, very humid and extremely humid. There seems to be a connection between the more humid classes and the territory's terrain with relatively high altitude. The very humid and extremely humid climates are therefore exhibited for the natural semi-mountainous and mountainous areas of higher altitudes (e.g., the arc of the Carpathians in RO, the Kopaonik Mountains in eastern RS, the Sharr Mountains in southern XK and eastern MK, the Rhodope Mountains in south BG and the Pindos Mountains range across mainland Greece). The humid and semi-humid classes characterize the lowland areas corresponding mainly to the inland agricultural plains (e.g., the humid Transylvanian and Moldavian Plains, respectively, in central and eastern RO, the semi-humid part of the Wallachian Plain in southern RO and both semi-humid and humid bioclimates of the Danubian Plain in northern BG). Overall, the less humid categories (Mediterranean and semidry) result mostly for the coastal (and lesser for the inland) lowland agricultural areas (e.g., the Mediterranean and semidry conditions of the Dobrujan Plateau and the Danube Delta area, respectively, in RO; the Thracian Plain's Mediterranean bioclimate in BG; and the semidry Attica area of central GR).

In addition, the resulting Mediterranean and semidry characterizations are most apparent for the eastern half of GR (eastern side of mountain ranges), with the latter category appearing, in general, more dominating.

The same IDM classes (semidry to extremely humid) result for the 1st period (2011–2040) under the RCP7 climate scenario (Figure 5). In general, minor differences in bioclimatic conditions may be expected for the PSEEU in relation to the reference period. An expansion of natural and agricultural areas with Mediterranean and semidry climatic characteristics at the expense of the more humid regime is foreseen by 2040 (e.g., for the Xanthi–Komotini Plain in north-eastern Macedonia, the Argolida Plain in north-eastern Peloponnese and the Vardar Valley in central MK). A slight reduction in the extremely humid with the increase in the very humid natural areas is also depicted for the investigated territory (e.g., for the western, southern Carpathians in RO and the Pindus mountains range and west Crete's White Mountains in GR). Moreover, the expansion of the areas with semi-humid bioclimatic conditions in place of those previously categorized as humid is evident for the northern areas of RS (Pannonian Plain) and western areas of RO (e.g., the west Crisana region).

Despite the IDM's distribution among the same categories as in the reference period (1981–2010) and the 1st period (2011–2040), a noticeable bioclimatic transformation for the 2nd period (2041–2070) under the RCP7 scenario is displayed in Figure 6. Significant warming and drying trends are exhibited over the entire PSEEU due to the expansion of the more xerothermic semidry, Mediterranean and semi-humid categories and the limited spatial pattern of humid, very humid and extremely humid categories. More semi-dry and Mediterranean, mainly agricultural areas are projected by 2070. This future evolution is noticeable in the agricultural areas of eastern and southern RO (e.g., Moldavian Plain, Dobrujan Plateau, Wallachian Plain), central eastern BG (e.g., Thracian Plain and Maritsa basin), northern and central GR (e.g., the plains of Thessaloniki, Serres, Drama, Xanthi–Komotini, Thessaly and Argolida) and Greek Aegean islands (e.g., Rhodes, Lesbos, Chios).

Moreover, a significant spatial occupation of the semi-humid and Mediterranean classes in place of the humid class results for the rural areas of northern and central RS and western RO.

The formation of a more dry thermal regime is also reflected by the noticeable reduction in extremely humid and very humid natural areas evidenced primarily in the Carpathian Mountains, western RS and MK, south-western BG and along the Greek Pindus Mountain range. It is highlighted that warmer and drier categories appear to characterize agricultural regions, for the first time, as in the case of semidry conditions in very limited southern Serbian areas and Mediterranean conditions in central and south-eastern XK.

A profound trend towards warmer and drier conditions is revealed for the future's long-term time frame (2071–2100) under the RCP7 scenario (Figure 7). An even higher spanning of semidry, Mediterranean and semi-humid characterizations accompanied by the spatial limitation in humid, very humid and extremely humid conditions is demonstrated. The spatial increase in the semi-dry and Mediterranean classes occurs for both natural and agricultural areas of the PSEEu, with the latter areas mainly being affected by more intense dry thermal conditions.

According to the results, these alterations in bioclimate are expected to follow the 2nd period's (2041–2070) geographical pattern. As such, more extensive xerothermic areas are now situated in the central, eastern, western and primarily southern plain agricultural areas of RO and BG; in northern, central and eastern RS; in northern, central, south-eastern XK and south-eastern and MK; and in, approximately, the eastern half of Greece. Regarding the previous periods, indications for the 3rd period's more enhanced dry thermal regime are based on the absence of extremely humid conditions in the agricultural areas of BG and GR and the presence—for the first time—of the dry category, with a very limited spatial pattern in Greece: in the Attica coastal areas of Kineta, Eleusina, Lagonisi; the Peloponnesian coastal area of Corinth; and the Santorini and Anafi Islands not distinguishable on the map of Figure 7 but visible in Figure S1 of the Supplementary Materials document. Furthermore, it is interesting to note that there is extended prevalence and clear dominance of semi-arid conditions in MK and GR, even at the expense of Mediterranean bioclimate conditions.

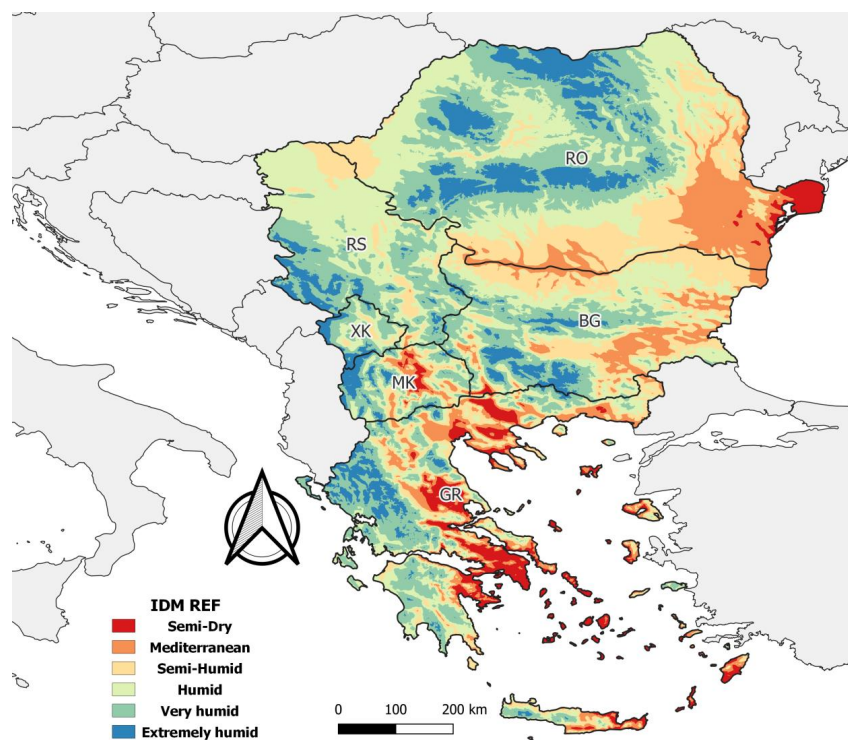


**Figure 4.** The de Martonne classes' spatial distribution during the reference (Ref) period: 1981–2010 (BG = Bulgaria; GR = Greece; MK = North Macedonia; RO = Romania; RS = Serbia; XK = Kosovo).

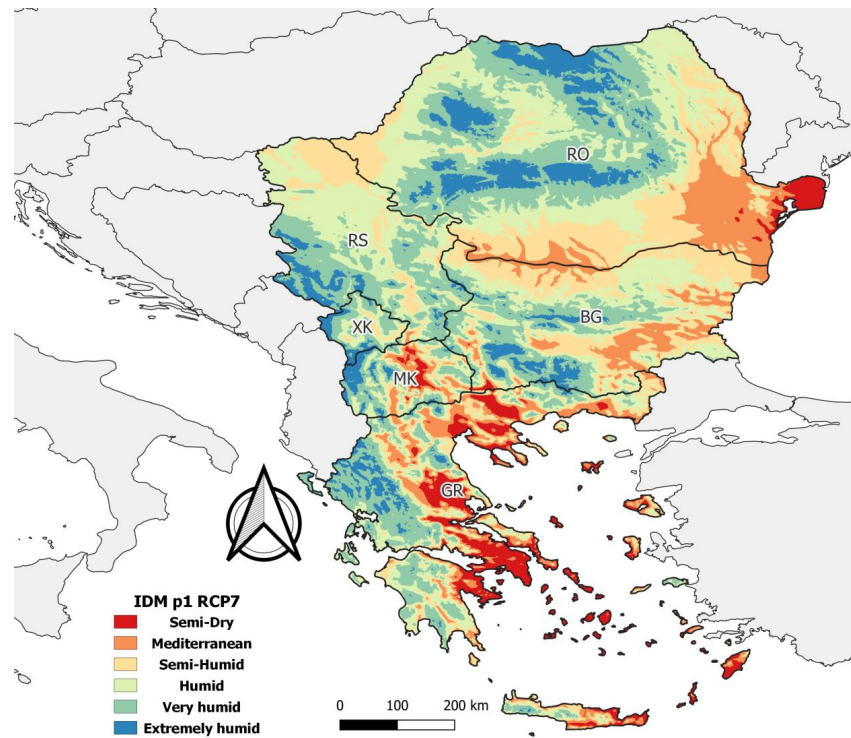


**Figure 5.** The de Martonne classes’ spatial distribution during p1 (2011–2040) in the RCP7 scenario (BG = Bulgaria; GR = Greece; MK = North Macedonia; RO = Romania; RS = Serbia; XK = Kosovo).

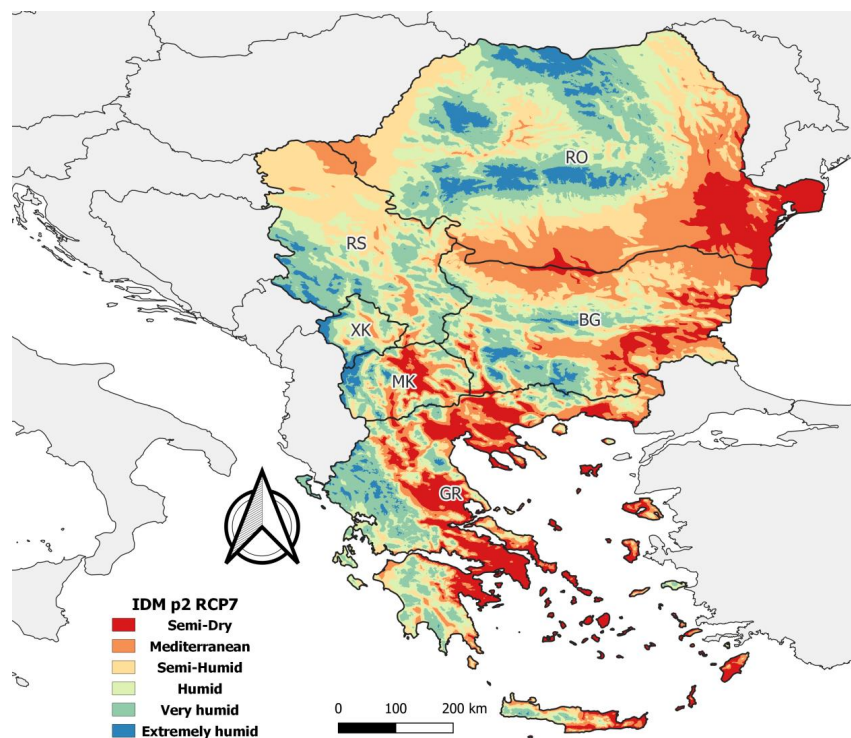


**Figure 6.** The de Martonne classes’ spatial distribution during p2 (2041–2070) under the RCP7 scenario (BG = Bulgaria; GR = Greece; MK = North Macedonia; RO = Romania; RS = Serbia; XK = Kosovo).

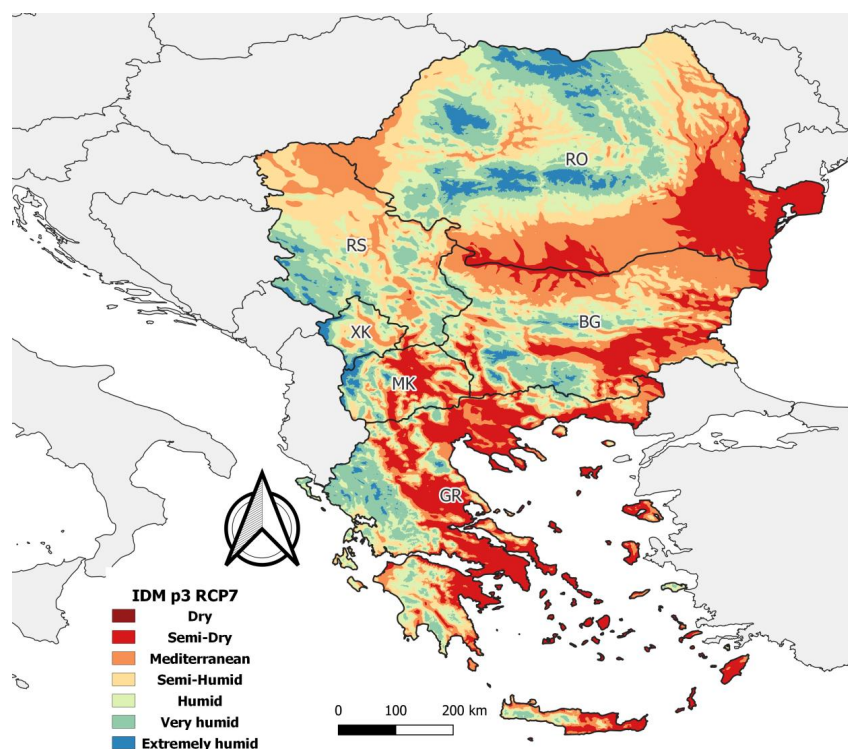


**Figure 7.** The de Martonne classes' spatial distribution during p3 (2071–2100) under the RCP7 scenario (BG = Bulgaria; GR = Greece; MK = North Macedonia; RO = Romania; RS = Serbia; XK = Kosovo).

As illustrated in Figure 8, for the extreme RCP8.5 scenario, the IDM is distributed among the same six classes as in the previous periods, including the respective RCP7 period. However, a spatial reduction in the drier categories (semidry, Mediterranean, semi-humid) may be distinguished regarding the latter scenario in favour of the more humid ones (humid, very humid, extremely humid).

This trend is depicted for southern, western, and eastern RO (e.g., Wallachian and Moldavian Plains); for northern RS, western XK and central MK (e.g., Vojvodina region, Metohija region, Vardar River Valley); for northern and central BG (e.g., Danubian and Thracian Plains); and northern GR (e.g., Xanthi–Komotini Plain). Overall, a rather similar IDM spatial pattern is evidenced compared with the reference period (1981–2010) except for GR and MK. Small spatial pattern increases of the semidry and Mediterranean classes are projected for both natural and agricultural areas in GR and an increase in the semi-humid class for the latter areas. As for MK, expansion of the areas with semidry to humid climates and of the first two categories (semidry and Mediterranean) are foreseen, respectively, for natural and agricultural areas.

The decrease in the areas characterized by drier conditions documented for the 1st period of RCP8.5 is not evidenced for the respective scenario's 2nd period (Figure 9). In this case, a reversed trend is documented, highlighting a warmer and drier bioclimatic regime with reference to the same time period as RCP7. Compared with RCP7, projections for RCP8.5 indicate a broader expansion of natural areas with semidry, Mediterranean and semi-humid climates and of the agricultural areas with semidry and Mediterranean climates for RO, BG, GR and MK. RS and XK also exhibit more intense xerothermic trends due to the expansion mainly of the Mediterranean and semi-humid natural and agricultural areas. Concerning the reference and 1st periods, more intense bioclimate alteration seems to occur over the entire PSEEu, with the drier categories' spatial patterns increases being more evident over agricultural areas. The appearance of Mediterranean conditions in both agricultural and natural areas of XK is also exhibited for the first time.

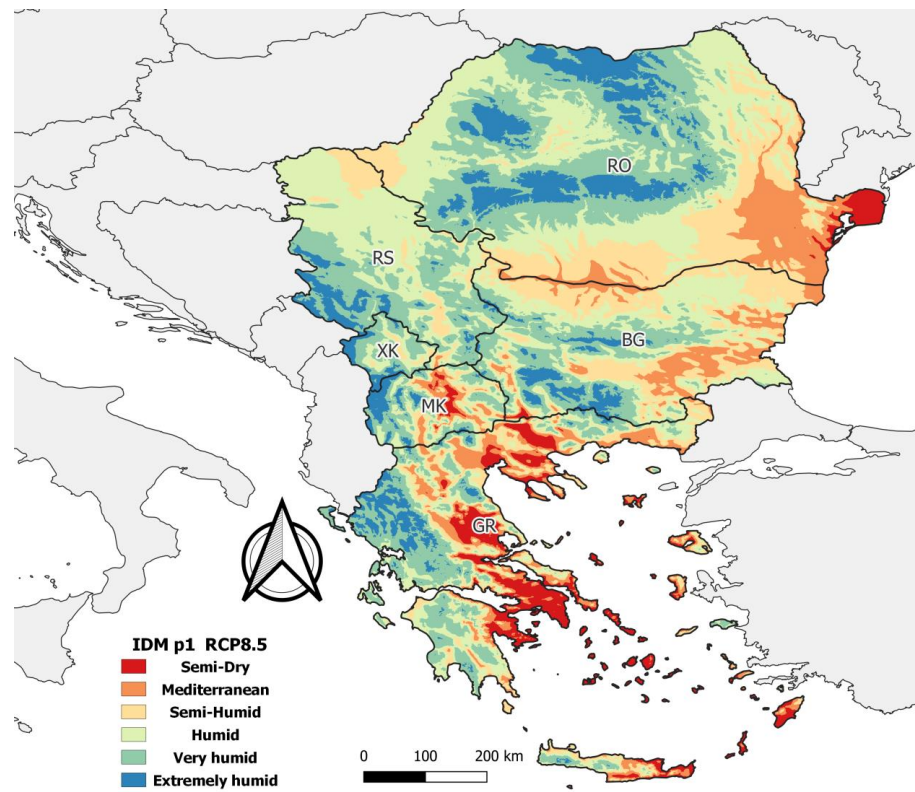


**Figure 8.** The de Martonne classes’ spatial distribution during p1 (2011–2040) in the RCP8.5 scenario (BG = Bulgaria; GR = Greece; MK = North Macedonia; RO = Romania; RS = Serbia; XK = Kosovo).

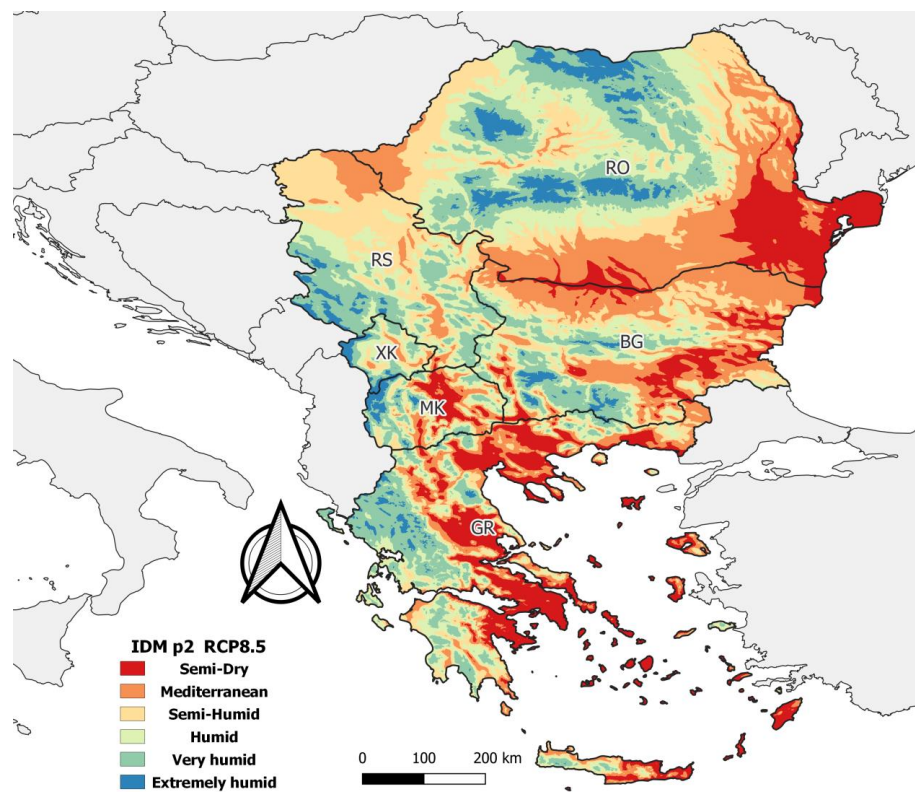


**Figure 9.** The de Martonne classes’ spatial distribution during p2 (2041–2070) under in RCP8.5 scenario (BG = Bulgaria; GR = Greece; MK = North Macedonia; RO = Romania; RS = Serbia; XK = Kosovo).

The 3rd period (2071–2100) of the RCP8.5 scenario appears as the most influential (Figure 10) considering the sizeable spatial pattern mainly of the semidry category, mostly over agricultural areas of RO, BG, GR and MK and the significant presence of a Mediterranean regime over natural areas of BG, GR and XK. As shown for RCP7, a remarkable prevalence of the semidry category is predicted for nearly the entirety of the eastern half of continental GR and GR's Aegean Islands, which, in the case of RCP8.5, corresponds to more extensive areas. A significant occupancy of MK by the semidry class is also expected by 2100. Furthermore, as in RCP7, semidry climatic conditions are likely to affect the natural and agricultural areas of XK and the latter areas in RS, but to a greater spatial extent. It is interesting to note the elimination of the extremely humid regime in the agricultural areas of BG and GR and the dominant appearance of the dry conditions' distribution in GR located in some more extended areas compared to those referred to in RCP7's respective period (areas Corinth in Peloponnese, the Aegean Islands and Attica including the coastal suburb of Vouliagmeni (not distinguishable on the map of Figure 10 but visible in Figure S2 of the Supplementary Material document).

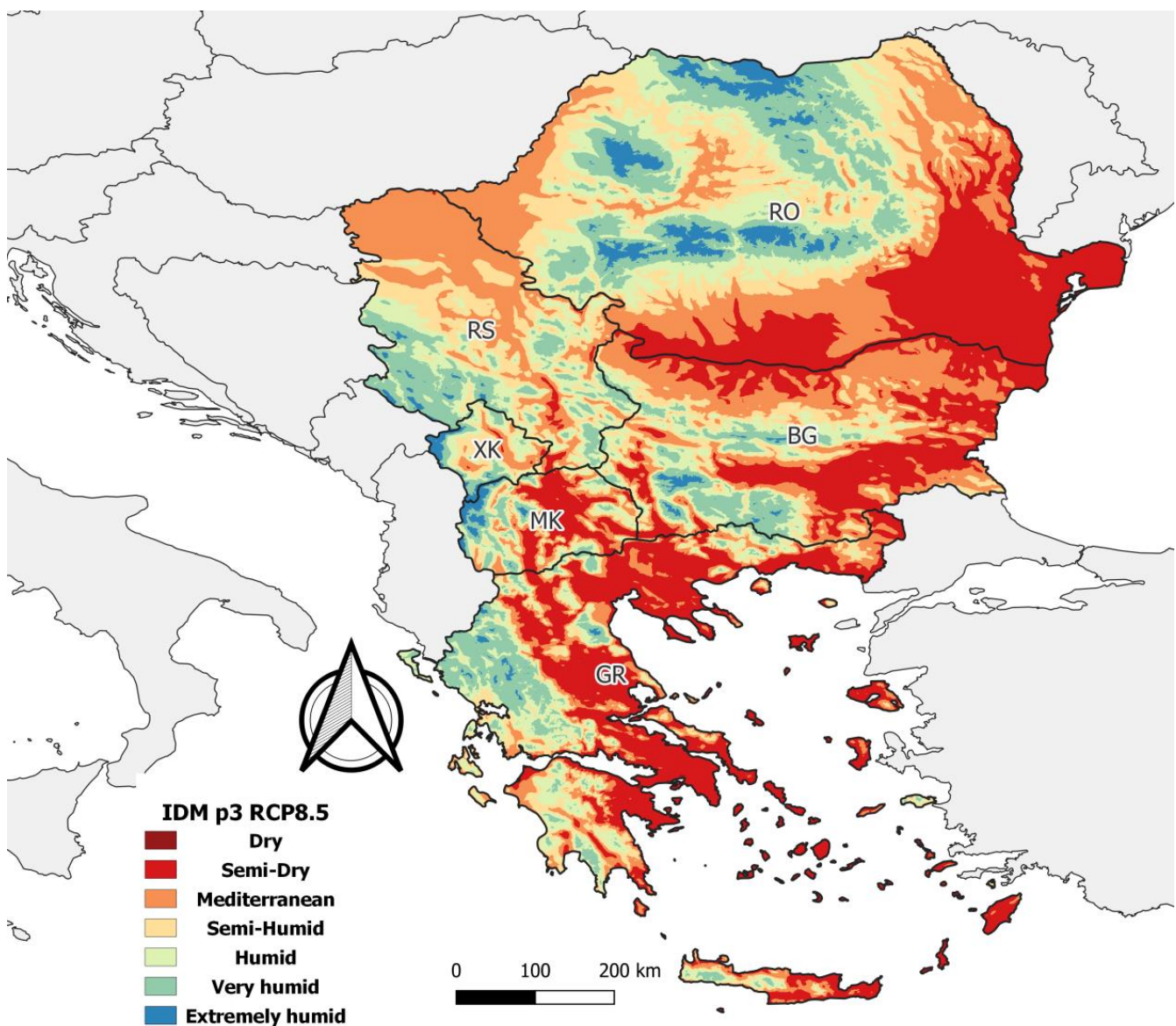


**Figure 10.** The de Martonne classes' spatial distribution during p3 (2071–2100) in the RCP8.5 scenario (BG = Bulgaria; GR = Greece; MK = North Macedonia; RO = Romania; RS = Serbia; XK = Kosovo).

By investigating the impact of a more optimistic RCP scenario (PRCP4.5), Nistor [8] also demonstrated the xerothermic trend over south-eastern Europe (area of the present study including the western coastal countries extending from Austria to Albania). With the exploitation of a relatively coarser resolution analysis (1 km<sup>2</sup>), the territory's bioclimate was also distributed among six de Martonne classes (semi-humid to extremely humid) for both of the investigated time periods: 2011–2040 and 2041–2070 (p1 and p2, respectively, of the present study).

Comparisons between the two periods revealed significant increases in the areas falling within the drier categories and most of the semidry and Mediterranean bioclimates. Despite the general agreement between Nistor's study and the present work's outcomes regarding the spatiotemporal evolution of the climate towards a more dry thermal regime, a significantly higher expansion of the drier areas was documented in the former study, exceeding the respective xerothermic footprint of the present study's case for p2 under the more "pessimistic" RCP8.5 scenario. In general, studies conducted in the same area have a high degree of agreement with the results of the present study both in the spatial distribution of the de Martonne index categories [8,13] and in the overall picture of drought trends [101].

### 3.2. The de Martonne Classes' Spatial Frequency over the PSEEU Countries

Figures 11–22 present the results on the relative frequencies of de Martonne's bioclimatic categories quantified over the natural and agricultural areas of the investigated territory's individual countries (in alphabetical order: Bulgaria, Greece, Kosovo, N. Macedonia, Romania, Serbia). For a more comprehensive description of the findings, the designations adopted include the reference period (Ref); the 1st, 2nd, and 3rd periods of RCP7 (p1 RCP7, p2 RCP7, p3 RCP7, respectively); and the 1st, 2nd and 3rd periods of the RCP8.5 emissions scenario (p1 RCP8.5, p2 RCP8.5, p3 RCP8.5, respectively).

#### 3.2.1. Bulgaria (BG)

Calculations of the relative frequency of IDM categories over the natural areas of BG (Figure 11) reveal a relatively similar pattern between the Ref and 1st periods of both scenarios (p1 RCP7 and p1 RCP8.5) with a slightly higher spatial reduction in the extremely humid areas in p1 RCP7 (10.9% vs. 11.7% in p1 RCP8.5 and 12.6% in the Ref). In comparison with the Ref, an increasing trend of the areas falling within the semidry, Mediterranean and semi-humid classes and the limitation of the areas with humid, very humid and extremely humid climatic characteristics is foreseen under both investigated scenarios (RCP7 and RCP8.5). Overall, the more intense xerothermic trend is depicted for p3 RCP8.5, given the maximization of the semidry and Mediterranean classes' distribution (15% in p3 RCP8.5 vs. 7.1% in p3 RCP7 for the semidry class and 27.3% in p3 RCP8.5 vs. 24.1% in p3 RCP7 for the Mediterranean class).

Raev et al. [57] focused on the fate of BG's forested areas impacted by the evolution of more arid conditions for the 2041–2060 and 2061–2080 intervals under four examined RCP emissions scenarios (RCP2.6, RCP4.5, RCP6.0 and RCP8.5). According to the IDM's estimations based on temperature and precipitation data with a relatively low spatial resolution (1 km<sup>2</sup>) and the adopted IDM classification scheme, a substantial sprawling of semiarid conditions (IDM values of 10–25) is projected to occur by 2070 over most of the Bulgarian territory for the RCP4.5 and RCP8.5 scenarios. Additionally, a significant part of the natural forested area, belonging to the "very high" vulnerability level, is expected to fall within the semiarid class (spatial distribution of 56.8% for 2041–2060 and of 65.6% for 2061–2080) under the RCP8.5 characterized thus as the most influential mainly during the 2nd investigated period.

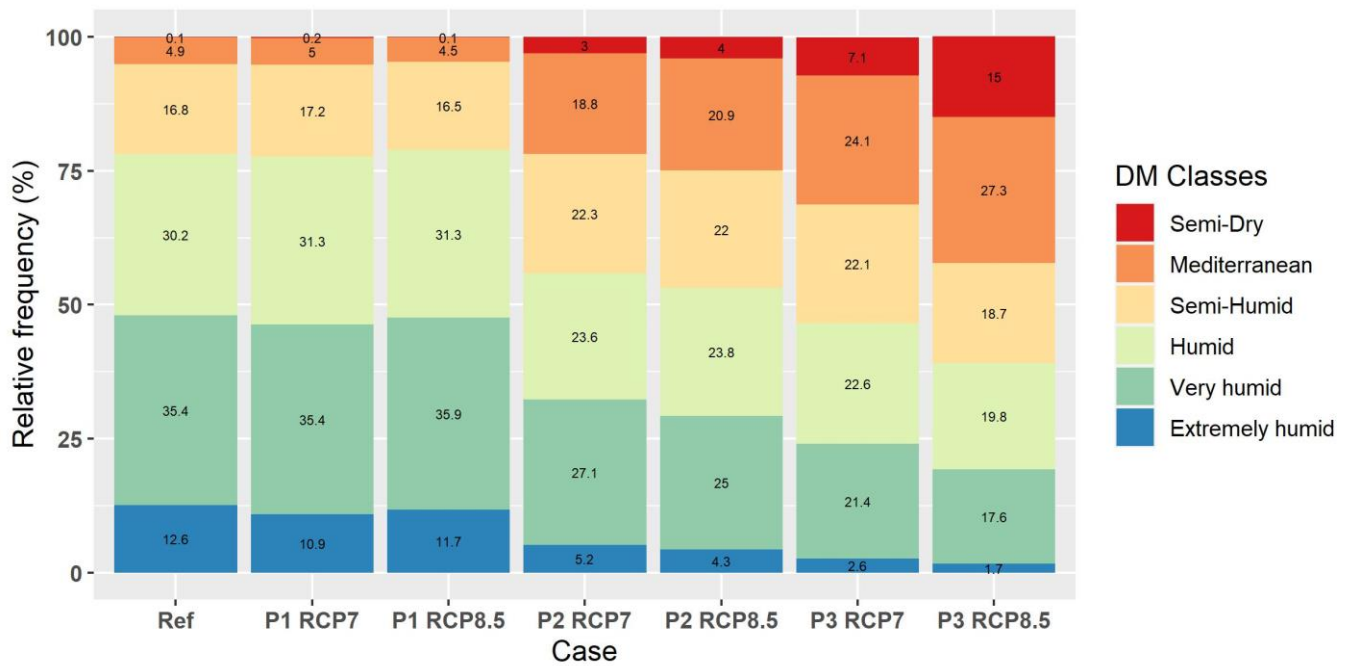


Figure 11. The de Martonne classes’ spatial relative frequency over the natural areas of Bulgaria.

For the first period of both scenarios, constant bioclimatic conditions are expected to occur over the agricultural areas of BG as demonstrated by the similar relative frequencies resulting for the Ref, p1 RCP7 and p1 RCP8.5 (Figure 12). A significant increase in the areas characterized by the semidry and Mediterranean climates is projected for p2 of both scenarios. However, the higher trend towards warmer and drier bioclimatic conditions is exhibited for p3 and under the extreme RCP8.5, where an almost doubling of the semidry agricultural areas is expected to occur (41.8% in p3 RCP8.5 vs. 22.7% in p3 RCP7). The severe impact of both scenarios on the agricultural areas’ alteration in bioclimate is denoted for p3, where the significant limitation and zeroing of relative frequencies in the very humid and extremely humid classes are foreseen.

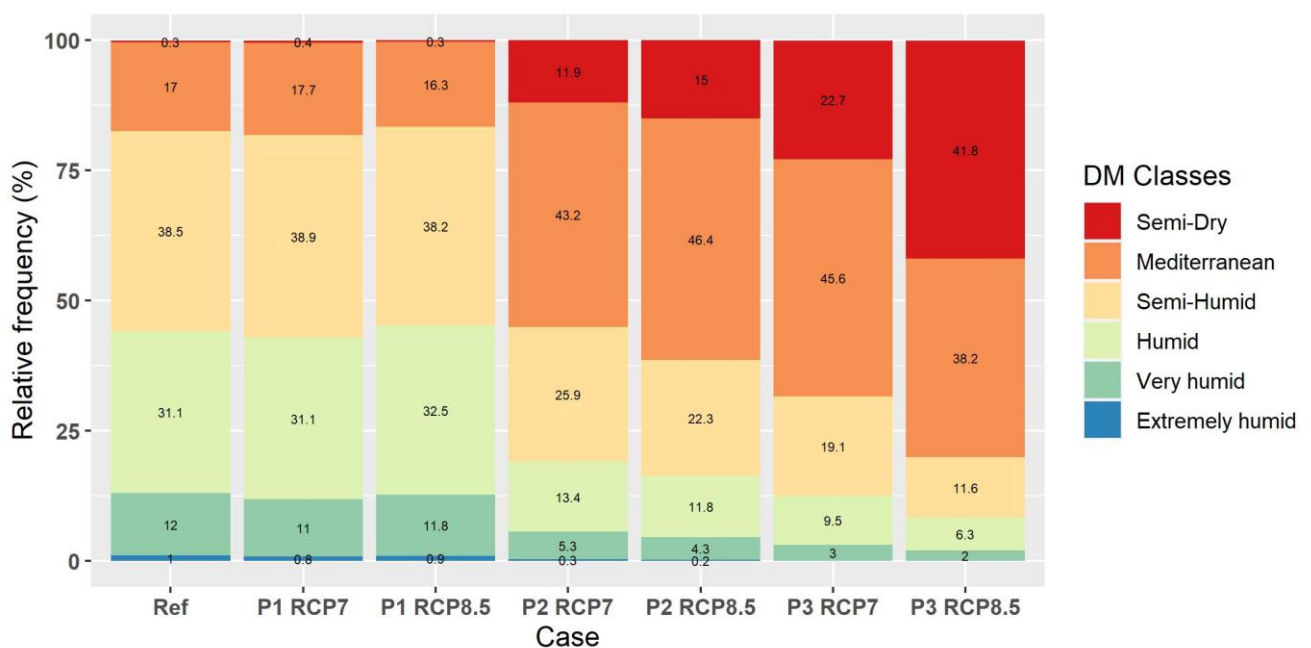


Figure 12. The de Martonne classes’ spatial relative frequency over the agricultural areas of Bulgaria.

Considering the potential bioclimatic evolution, it becomes evident that the long-term water requirements for agricultural production will increase significantly in BG and involve both irrigation (under the semidry regime) and supplementary irrigation (under the Mediterranean regime).

### 3.2.2. Greece (GR)

The relative frequency of IDM classes over the natural areas of GR is presented in Figure 13. Similar patterns regarding bioclimatic categories result between the Ref, p1 RCP7 and p1RCP8.5, excluding the higher (lower) relative frequency of the semidry (extremely humid) classes in RCP7 (e.g., 7.3% in p1 RCP7 vs. 10.1% in Ref and 9% in p1 RCP8.5). For both examined scenarios, trends towards a warmer and drier bioclimate are depicted for p2 and p3 given the (gradual) increase in the semidry, Mediterranean and semi-humid natural areas and the decrease in the humid, very humid and extremely humid areas. The extreme RCP8.5 scenario emerges as the more impactful scenario, especially in p3, where semidry conditions prevail in rather extended areas (percentage area of approximately 34%), followed by Mediterranean conditions (percentage area of nearly 19%). In addition, during this period, very limited natural areas are projected as being impacted by the effects of the most xerothermic dry conditions (very narrow area of 0.1%).

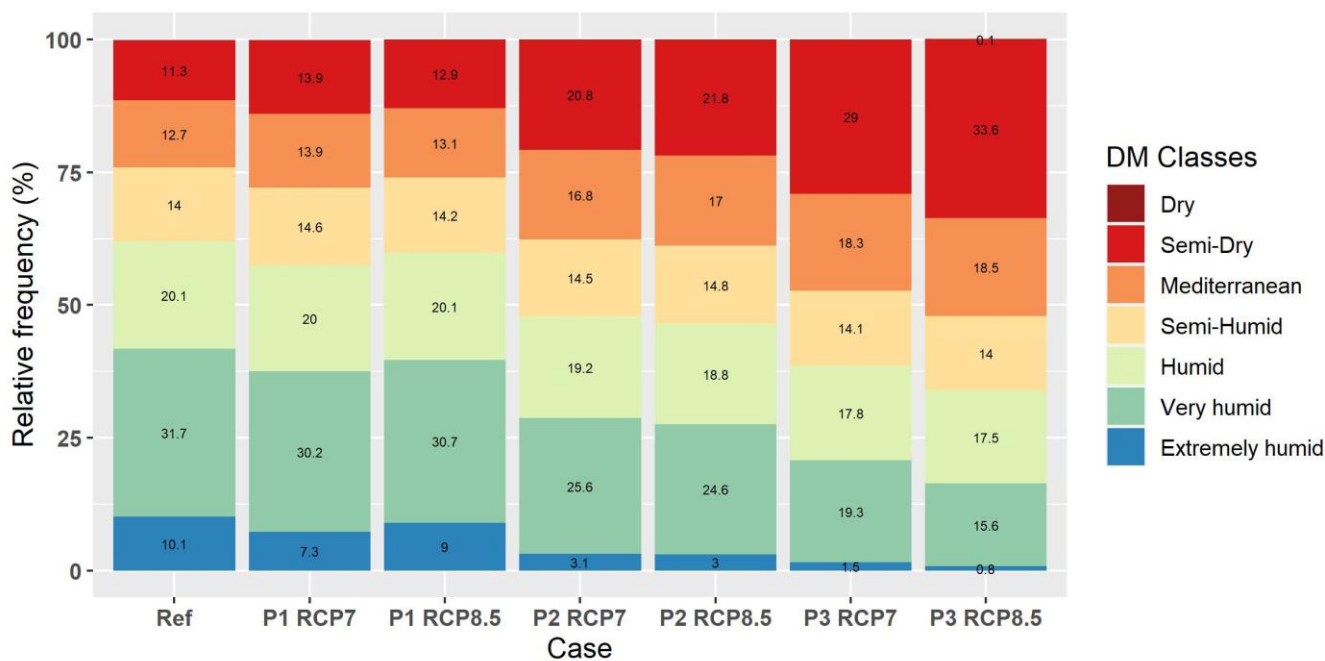


Figure 13. The de Martonne classes’ spatial relative frequency over the natural areas of Greece.

Increases in the drier classes’ (semidry, Mediterranean) spatial distribution in place of the more humid classes occur in all periods of both investigated scenarios for the agricultural areas of GR (Figure 14). This is not the case for p2 RCP7, where a slight reduction in the Mediterranean category’s relative frequency is shown (24.4% in p2 RCP7 vs. 25.3% in p1 RCP7). In general, the agricultural areas exhibit a profound trend towards a more dry thermal regime where the predominance of the semidry category is foreseen by 2100 (frequencies of 53.9% and 60%, respectively, for the RCP7 and RCP8.5 emissions scenarios). In addition, the diminishing of the extremely humid regime and the occurrence of dry bioclimatic conditions (dry class’s frequency of 0.2% and 0.3% in RCP7 and RCP8.5, respectively) take place in p3 of both scenarios.

Furthermore, it should be emphasized that a substantial part of the agricultural areas, which is expected to be characterized by semidry bioclimatic conditions (53.9% in p3 RCP7 and 60% in p3 RCP8.5), will depend on irrigation water supply, and many areas corresponding to the Mediterranean regime (approximately 20% for both scenarios) will

need supplementary irrigation. This evolution under the RCP7 and RCP8.5 scenarios raises concerns about the fate of the agricultural sector in GR when also considering the introduction of the most xerothermic “dry” bioclimatic conditions; this, in turn, might have severe impacts on the country’s production capacity keeping in mind the far future’s excessive water requirements.

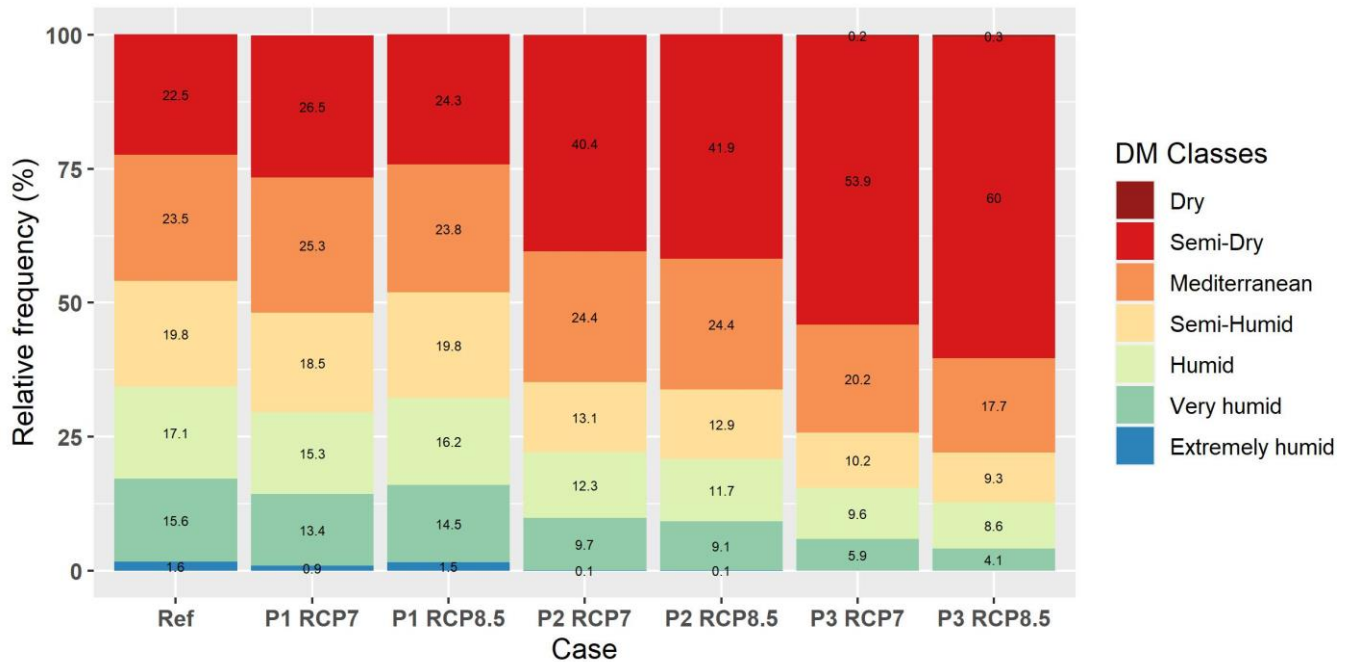


Figure 14. The de Martonne classes’ spatial relative frequency over the agricultural areas of Greece.

### 3.2.3. Kosovo (XK)

According to Figure 15, the Mediterranean class describes the bioclimatic footprint of XK’s natural areas as extremely humid bioclimates during all periods of both scenarios and for the additional semidry category only in p3. The humid, extremely humid, and mainly very humid bioclimates dominate the areas initially in p1 (the very humid class’s frequency of 48.4% and 50.9% for p1 RCP7 and p1 RCP8.5, respectively) and are gradually substituted by the drier semi-humid and Mediterranean regimes. These changes are more pronounced under the extreme RCP8.5 scenario and especially for the long-term timespan where higher patterns of semi-humid (24.1% vs. 20.9% in p3 RCP7 and 2.2% in the Ref), Mediterranean (9.2% vs. 6.4% in p3 RCP7) and semidry (0.4% vs. 0.1% in p3 RCP7) bioclimates are expected.

The evolution scheme towards a drier and warmer bioclimate of the XK’s agricultural areas is shown in Figure 16. Projections for both scenarios and mainly for the RCP8.5 reveal the dominance of the humid and very humid categories in p1 (e.g., 44.7% and 40%, respectively, for the humid and very humid categories in RCP8.5). These classes are expected to be consecutively substituted by the drier Mediterranean (more than twofold expansion in p3 vs. p2) and semi-humid (almost threefold in p3 vs. in Ref), which are shown to prevail to a substantial areal extent by the end of the century (64% in total of the Mediterranean and semi-humid areas vs. 32.6% of the humid and very humid areas in p3 RCP8.5). The other driest regime corresponding to the semi-dry category is expected to impact limited areas in the long term in RCP7 and mainly RCP8.5 scenarios (2.9% in p3 RCP8.5 vs. 0.4% in p3 RCP7). The dominance of Mediterranean and semi-humid bioclimates under both scenarios by 2100 points to the requisite scheduling for supplementary irrigation of agricultural areas in XK.

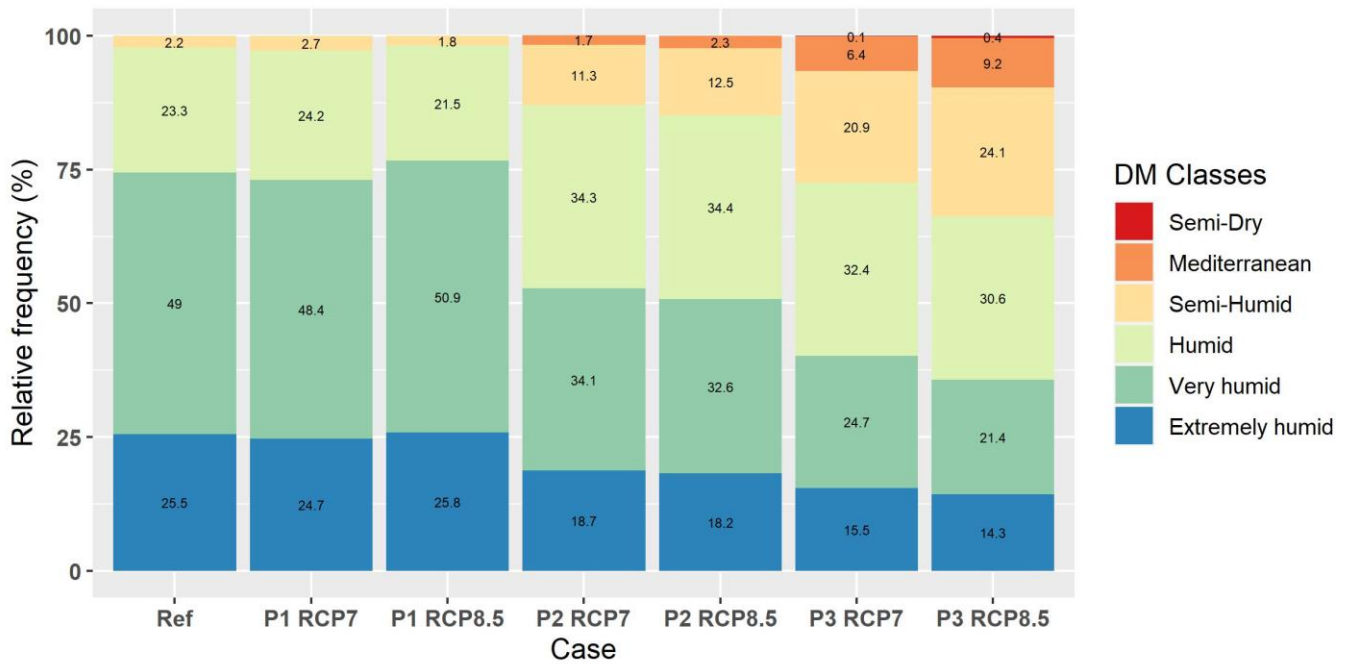


Figure 15. The de Martonne classes’ spatial relative frequency over the natural areas of Kosovo.

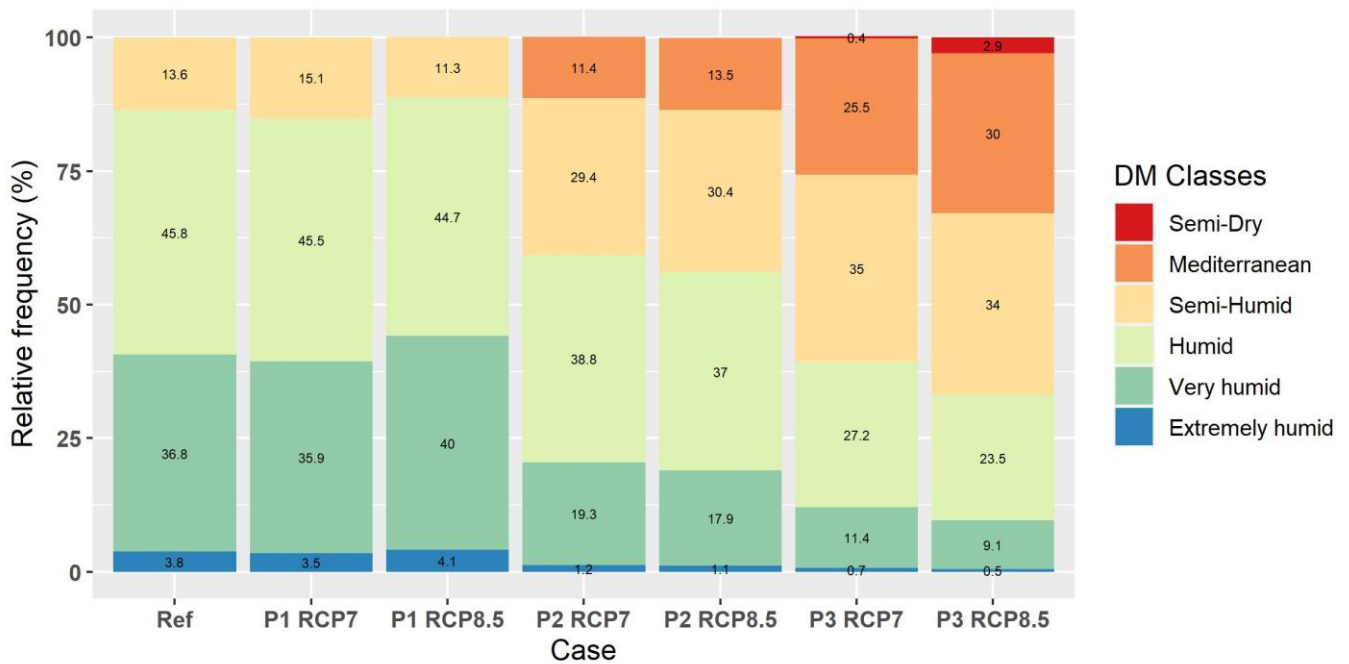


Figure 16. The de Martonne classes’ spatial relative frequency over agricultural areas of Kosovo.

### 3.2.4. North Macedonia (MK)

Concerning the Ref, results for the natural formations of MK show a general future expansion of semidry, Mediterranean and semi-humid areas at the expense of the humid, very humid and extremely humid conditions in both examined scenarios (Figure 17). The natural MK regions are expected to be slightly more impacted by RCP7 compared with RCP8.5, but only in p1, due to the moderately broader pattern of the drier classes (e.g., 8.3% in p1 RCP7 vs. 7.6% in p1 RCP8.5 and 7.2% in the Ref, for the Mediterranean class). Concerning the reference period, the xerothermic trend is more evident for the RCP8.5

scenario and to a great degree in p3, given the highest occupancy mainly by the semi-dry class (16% vs. 1.4% in the Ref).

Moreover, it is found that the Mediterranean (18.7% vs. 7.2% in the Ref) class covers the natural areas in place of the humid (21.8% vs. 23% in the Ref) and mainly very humid (18% vs. 38.6% in the Ref) and extremely humid areas (7.4% vs. 18.8% in the Ref).

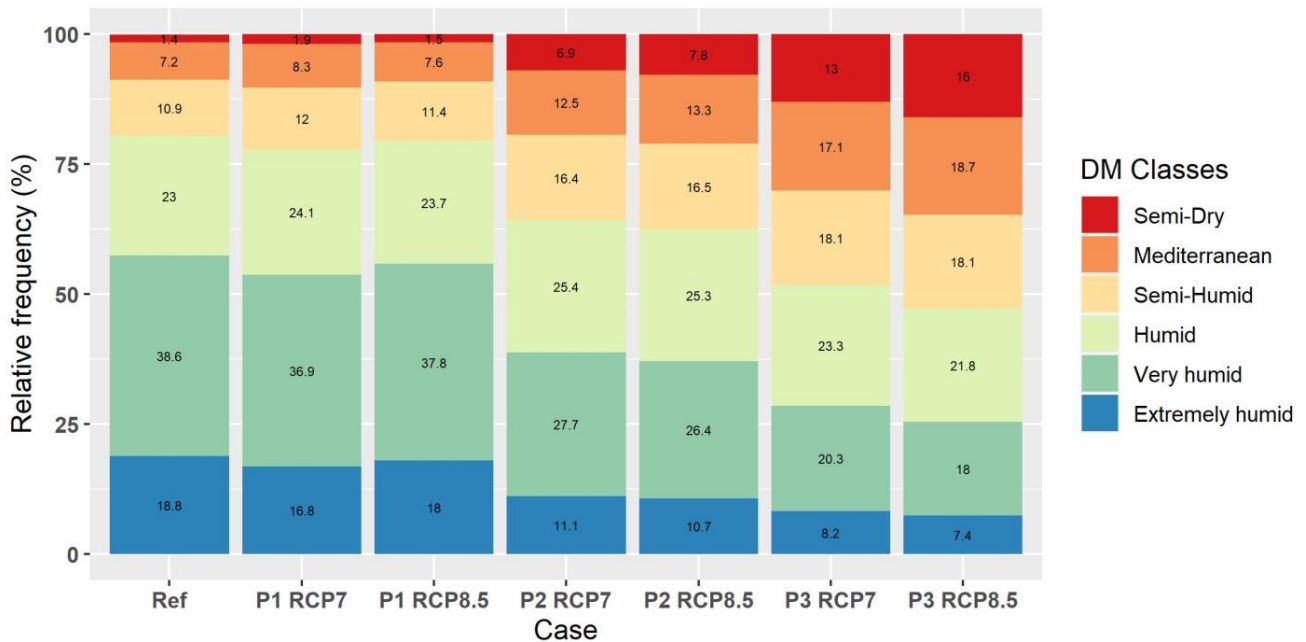


Figure 17. The de Martonne classes’ spatial relative frequency over the natural areas of North Macedonia.

A significant alteration in the agricultural areas’ future bioclimate in MK is illustrated in Figure 18. An overall dominance of the semidry and Mediterranean classes is demonstrated for both scenarios in p2 and p3, with a peaking of the xerothermic trend denoted for the latter period.

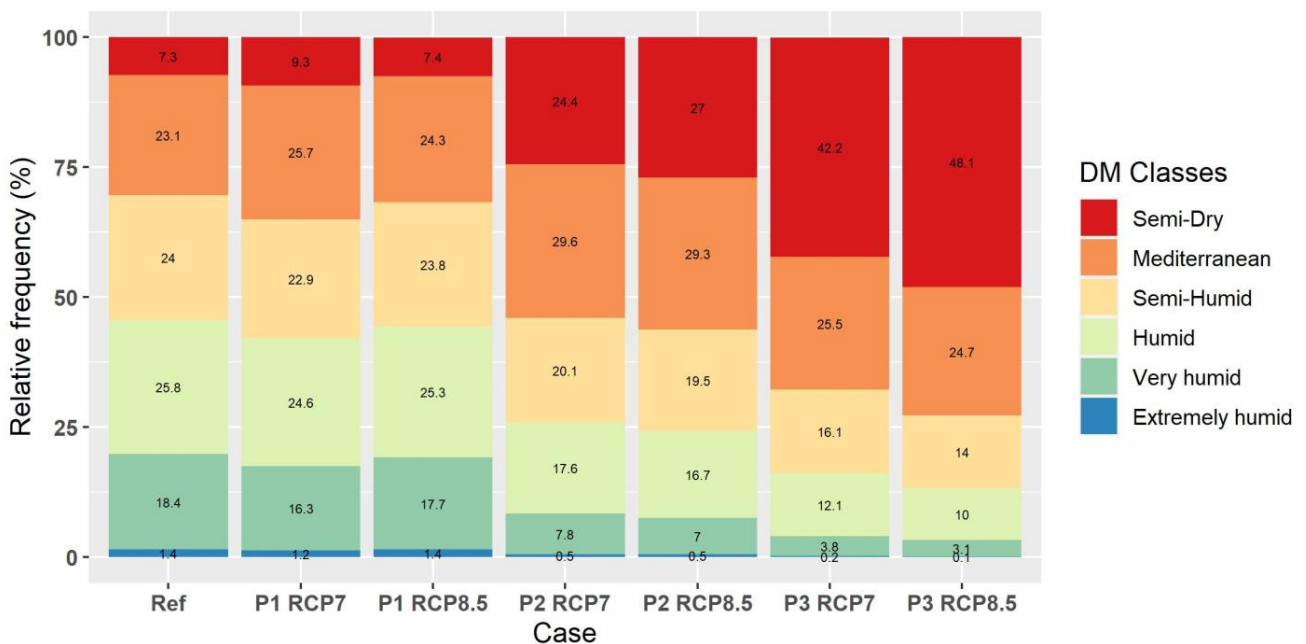


Figure 18. The de Martonne classes’ relative frequency over the agricultural areas of North Macedonia.

The driest semidry category, in particular, exhibits the highest relative frequencies in RCP7 (sixfold expansion of 42.2% vs. 7.3% in the Ref) and to a larger extent in RCP8.5 by occupying approximately half (48.1%) of the agricultural areas of MK. These potential developments are accompanied by the severe limitations of the humid and mainly very humid class (3.1% in p3 RCP8.5 vs. 18.4% in the Ref) and the elimination of the extremely humid class (0.1% in p3 RCP8.5 vs. 1.4% in the Ref).

The more intense xerothermic regime formed by semidry conditions will probably enforce higher irrigation demands for the sustainability of MK’s agriculture. The need for supplementary irrigation will also be raised by 2100, considering the substantial spatial pattern of the Mediterranean conditions (25.5% and 24.7% in p3 RCP7 and p3 RCP8.5, respectively).

### 3.2.5. Romania (RO)

The bioclimates’ relative frequencies over the natural areas of RO are shown in Figure 19. Similar IDM class patterns can be seen by comparing Ref and p1 for both scenarios with minor differences in RCP7 under which more limited natural areas associated with the extremely humid class are expected (25.9% vs. 28.6% in p1 RCP8.5 and 28% in the Ref). A trend towards warmer and drier conditions is evident for both scenarios’ consecutive p2 and p3 time frames, with the extreme scenario displaying a more substantial impact. Thus, results of p3 RCP8.5 depict more limited relative frequencies of the very humid and mainly of the extremely humid class (11.1% vs. 13.5% in p3 RCP7 and 28% in the Ref) accompanied by the higher occurrence of the semidry, Mediterranean and most of the semi-humid class (17% vs. 13.3% in p3 RCP7 and 4.8% in the Ref). A general humid regime, however, is present at the end of the century even for the extreme scenario, given that the humid to extremely humid categories prevail with a total relative frequency of 69.3%.

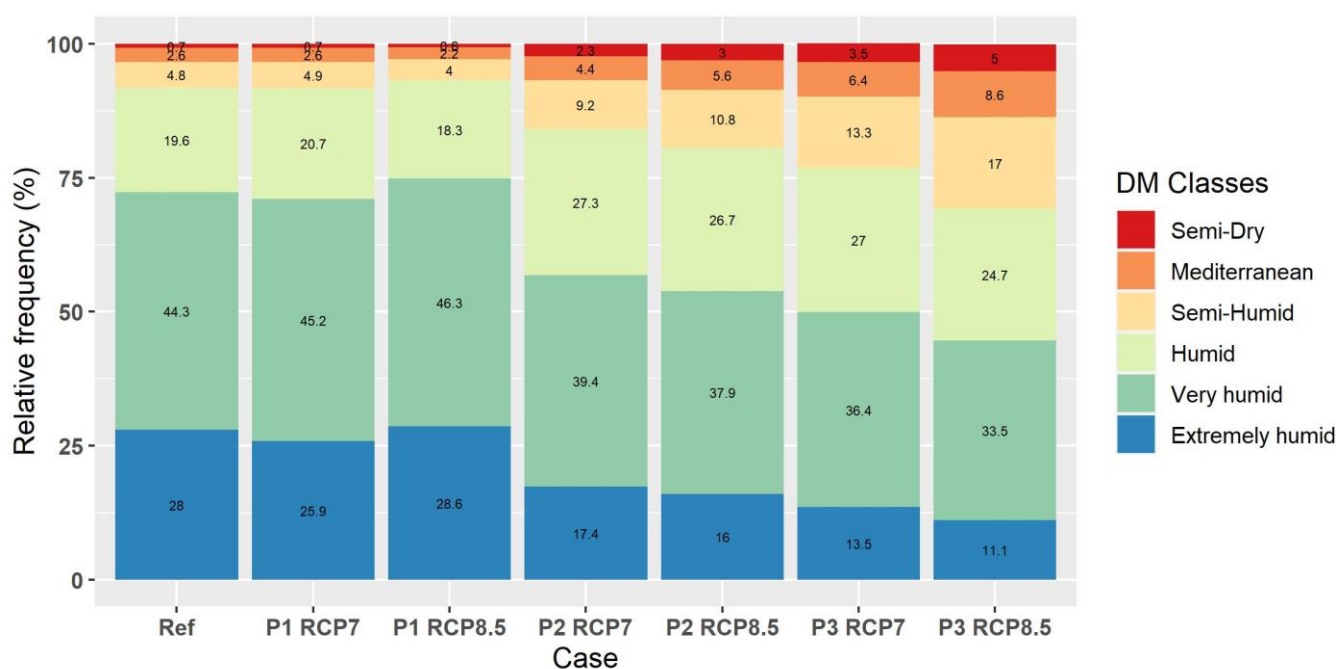


Figure 19. The de Martonne classes’ relative frequency over the natural areas of Romania.

As shown in Figure 20, the agricultural areas’ change in bioclimate is projected in general for both investigated scenarios in RO. Concerning the Ref, a slight increase in the humid class’s frequency is demonstrated for p1 RCP7 and in the humid to extremely humid classes for p1 RCP8.5 (e.g., 25% vs. 21.9% in p1 RCP7 and 22.8% in the Ref, for the very humid category). The highest agricultural areas characterized by a semi-dry bioclimate is exhibited for the latest period under the extreme RCP8.5 (27.2% vs. 17.3 in p3 RCP7 and 1% in the Ref) at the expense of all remaining categories.

By 2100 and under the RCP8.5 scenario, relatively broad areas are expected to be impacted by semidry (27.2%) and Mediterranean (26.7%) bioclimatic conditions, thus subjecting agricultural productivity to severe dependence on irrigation (semidry bioclimate) or supplementary irrigation (Mediterranean bioclimate).

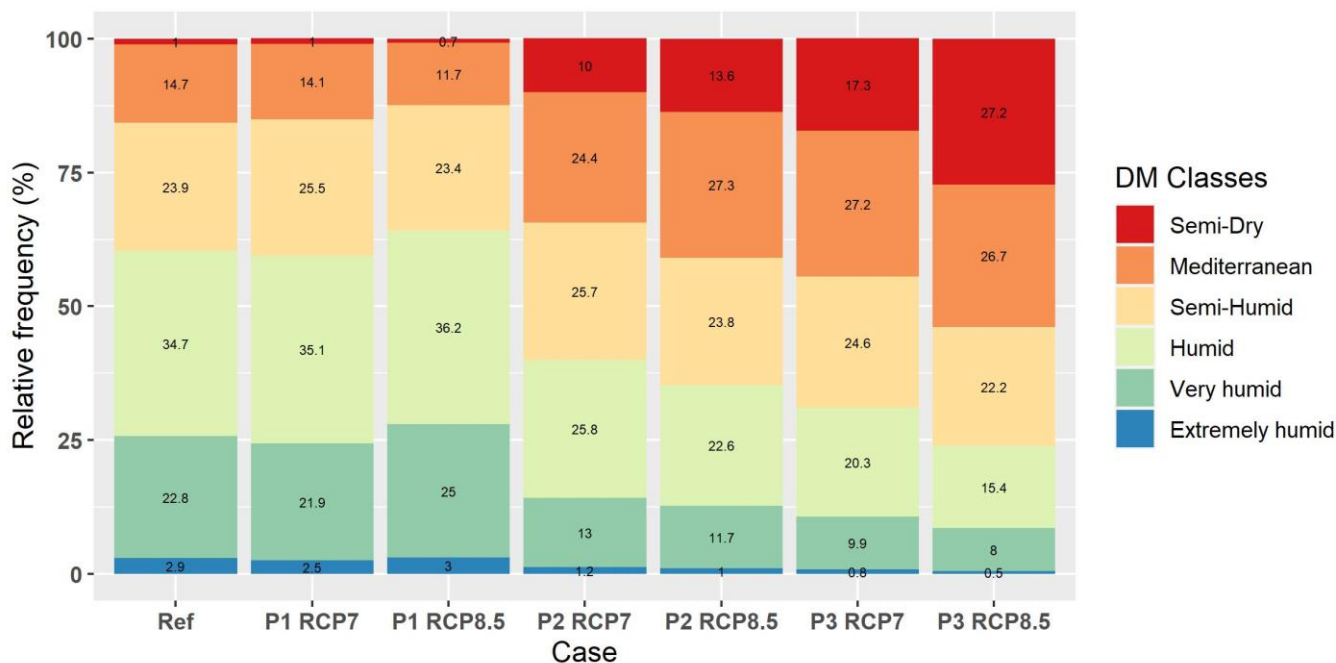


Figure 20. The de Martonne classes’ relative frequency over the agricultural areas of Romania.

### 3.2.6. Serbia (RS)

Throughout the examined periods for the scenarios examined, RS’s natural areas fall within the Mediterranean to extremely humid classes (Figure 21), excluding p3, where very few areas are identified as semidry (0.2% in p3 RCP7 and 0.7% in p3 RCP8.5). The more xerothermic bioclimate evidenced in p2 and mostly in p3, for both scenarios, is demonstrated by the Mediterranean to humid classes’ relative frequency increase (e.g., 14.9% in p3 RCP8.5 vs. 5% p2 RCP8.5 and 0.1% in both p1 RCP8.5 and the Ref, for the Mediterranean category) and the decreases in the very humid and extremely humid classes (e.g., 2% in p3 RCP8.5 vs. 6.7% in p2 RCP8.5 vs. 15.1% in p1 RCP8.5 and 14.9% in the Ref, for the extremely humid category). Between scenarios, the drier condition results are dominant for p3 RCP8.5 mainly due to an almost twofold relative frequency increase in the Mediterranean class (14.9% vs. 8.2% in p3 RCP7) and to the more than respective threefold increase in the semidry class (0.7% vs. 0.2% in p3 RCP7).

As illustrated in Figure 22 for the agricultural areas of RS, the change towards a more dry thermal regime is denoted for both scenarios by the sprawling of the areas foreseen as being impacted by Mediterranean and semi-humid conditions and shrinkage in the areas falling within the humid to extremely humid categories.

The maximization in the spatial distribution of the more arid conditions (represented by the semidry and Mediterranean classes) is depicted for p3, where RCP8.5 demonstrates a more critical impact than RCP7. This is outlined by a profound almost doubling of the areas projected as being influenced by Mediterranean conditions under RCP8.5 (47.6% in p3 RCP8.5 vs. 26% in p3 RCP7) along with the presence of more than threefold semidry areas (1.8% in p3 RCP8.5 vs. 0.5% in p3 RCP7). The increased xerothermic trend projected for p3 RCP8.5, mainly due to the significant expansion in the Mediterranean class (47.6% vs. 14% in p2 RCP8.5 and 0.3% in the Ref), highlights the possible future supplementary irrigation crop requirements in RS.

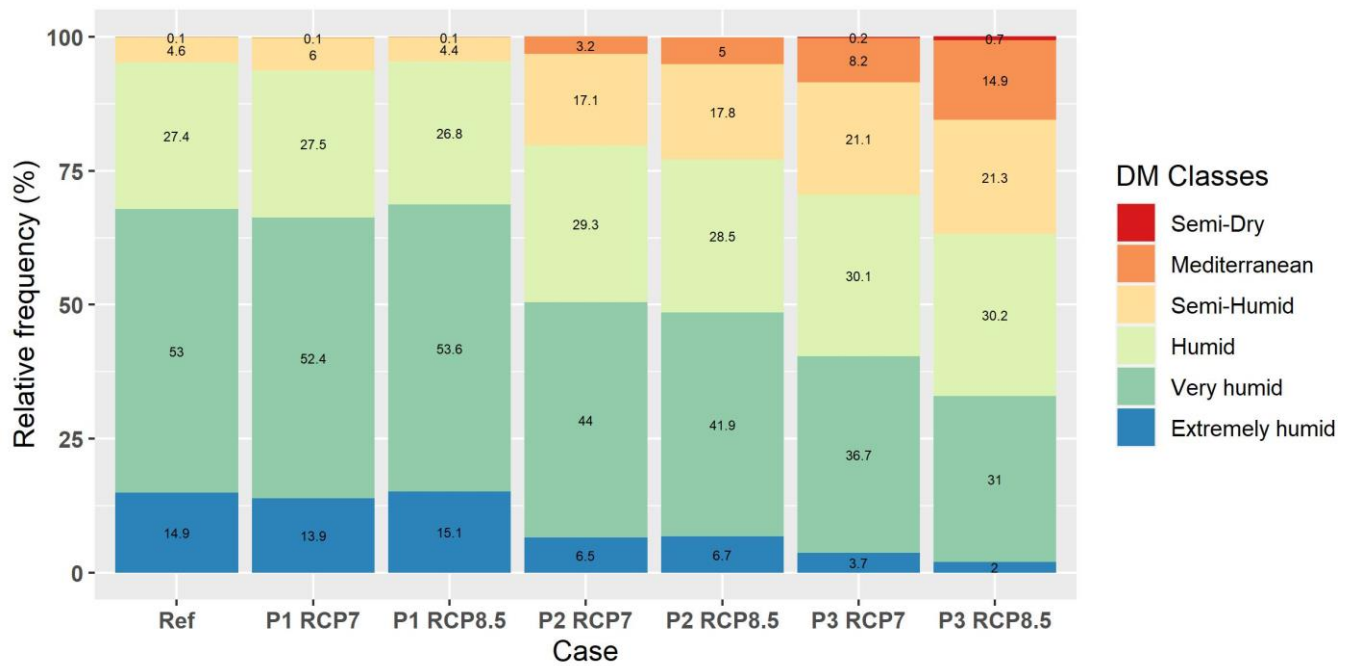


Figure 21. The de Martonne classes’ spatial relative frequency over the natural areas of Serbia.

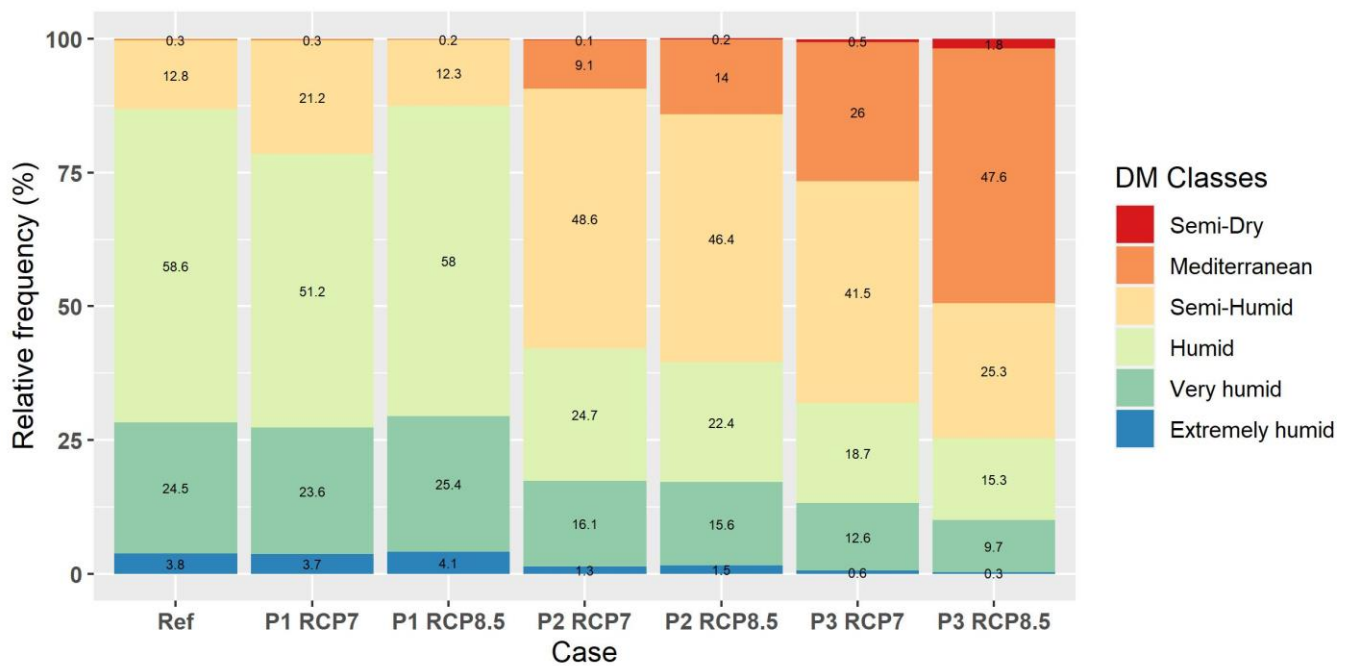
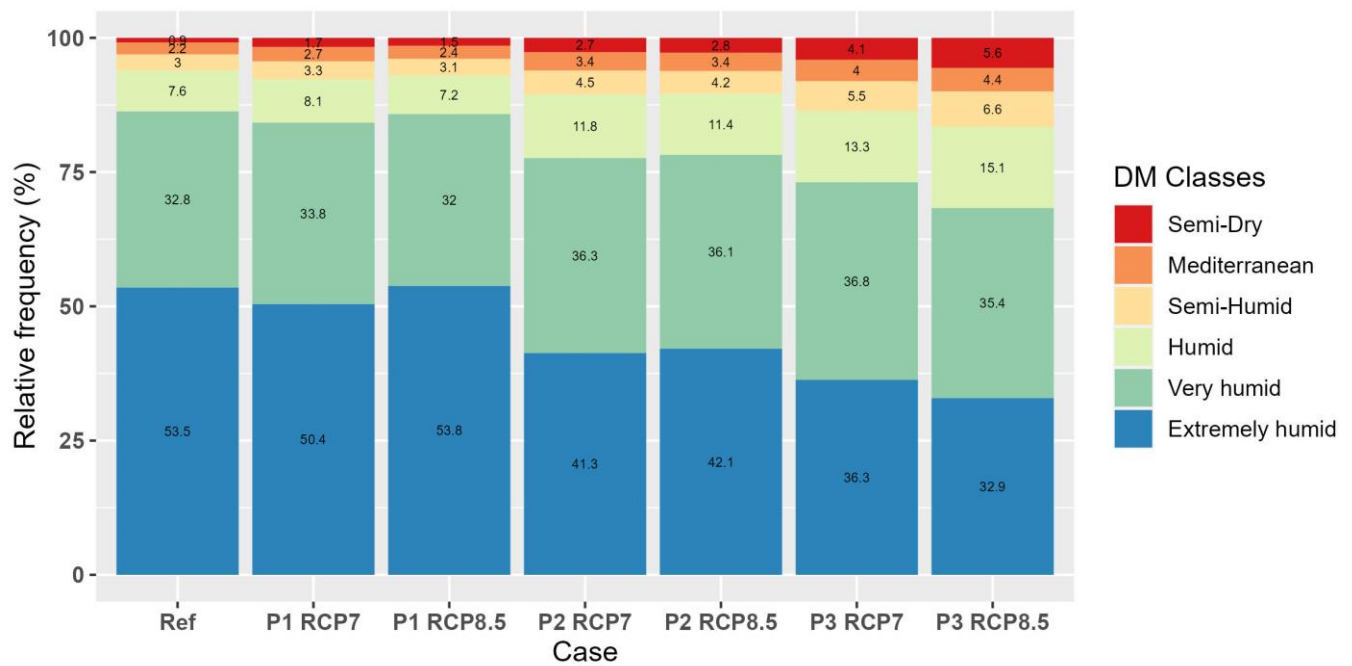


Figure 22. The de Martonne classes’ spatial relative frequency over the agricultural areas of Serbia.

### 3.2.7. Total Area de Martonne Classes Spatial Frequency

To make an overall assessment of the studied area, spatial statistics were calculated for its entirety in terms of both natural and agricultural areas (Figures 23 and 24). In general, the PSEEU will face more xerothermic conditions in the future under climatic conditions of the examined greenhouse emissions scenarios. More specifically, the driest class (semidry), which was negligible (0.9%) during the reference period, would reach and surpass the 5% mark during the 3rd period under the RCP8.5 scenario.



**Figure 23.** The de Martonne classes’ spatial relative frequency over the natural areas of the study area.

The relative surface, which is covered by the very humid class, is almost steady between the examined cases when the drier classes (humid, semi-humid, Mediterranean and semidry) rise. On the other hand, the more wet class, extremely humid, reduces as we move to the future in the highest emissions scenarios.

The pattern of relative frequencies of de Martonne classes of agricultural areas (Figure 24) reveals an amplified xerothermic projection. We can assume that it is a consequence of the lower altitudes of the agricultural areas in contrast to the frequently mountainous regions of the natural areas (there is a positive relationship between higher altitudes and lower air temperature, and higher precipitation). Thus, we can pinpoint that the humid class is almost steady in relative humidity, and the drier classes (semi-humid, Mediterranean and semidry) increase. In contrast, the wetter classes, such as very humid and extremely humid, decrease.

It is worth mentioning that the semidry class could triple its relative surface from the reference period to RCP8.5 p3, and the extremely humid class could triple down for the same period and scenario. Thus, these projections mean that some crop types should change soon in order to be viable and sustainable. The presented research has some limitations. The main one is that the input data, and therefore the results presented, relate to thirty-year averages. This means that there are no outliers (maxima and minima) that have a very large impact on ecosystems and crops. This could be improved using a dataset derived from annual data. Another limitation concerns the presentation of spatial statistics. For reasons of publication size, we presented the data by country. It would be very useful to present spatial statistics showing the likely bioclimatic change for specific, important natural and agricultural areas within countries.

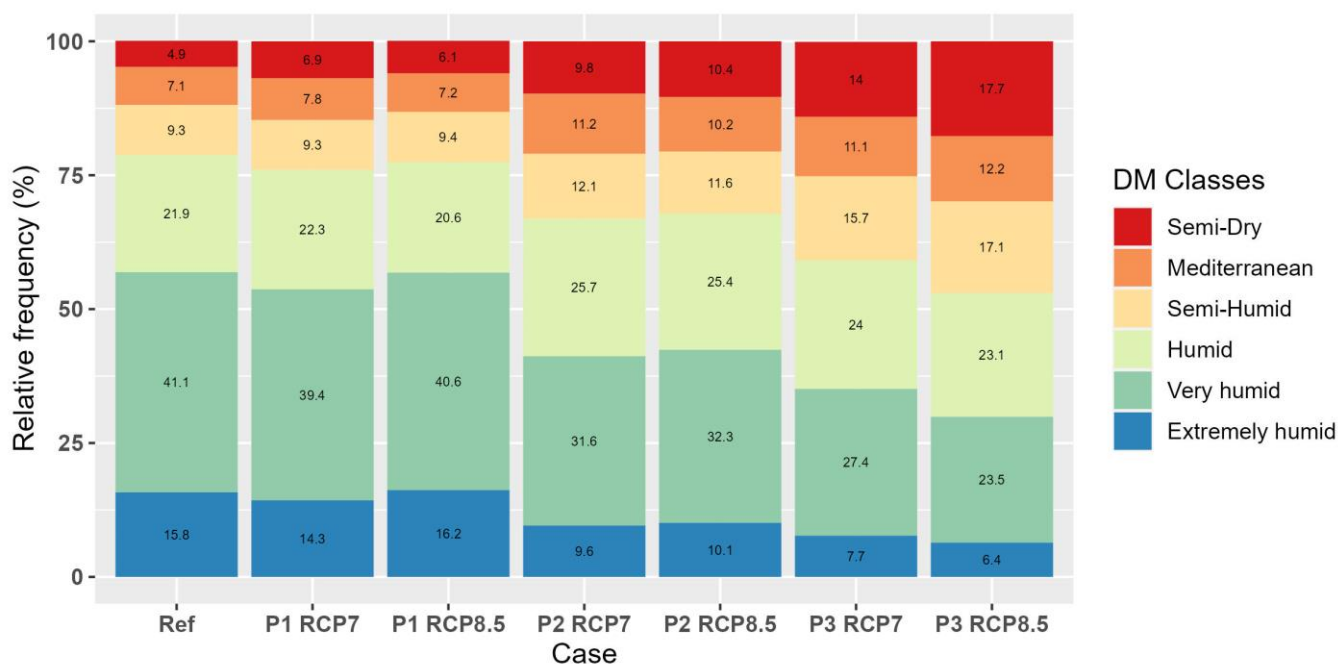


Figure 24. The de Martonne classes’ spatial relative frequency over the agricultural areas of the study area.

#### 4. Conclusions

The present study’s outcomes highlight the altered bioclimatic footprint depicting a more xerothermic regime by 2100. The above is apparent for the natural and agricultural areas appearing over the entire investigated section of south-eastern Europe under the RCP7 (SSP370) and RCP8.5 (SSP858) scenarios.

Profound trends towards warmer and drier conditions are demonstrated for the future’s long-term time frame (2071–2100) under RCP7 and mainly under the extreme RCP8.5 scenario.

By the end of the 21st century, the more prominent influence of the RCP8.5 scenario is expected to be evidenced by the vulnerable semidry, primarily agricultural areas situated in the lowland zones of Bulgaria, Greece, N. Macedonia and Romania.

Potential expansion of natural areas impacted by Mediterranean bioclimatic conditions is projected for the above countries, and particularly for Kosovo and Serbia, where more agricultural areas will also be influenced in the far future.

Greece appears as a particularly affected region in proportion to its total spatial area, given that the predictions show that semidry conditions will prevail over approximately half of the country, e.g., in the Natura 2000 network sites and/or at sites of endemic taxa or ecosystem services, for which special management is needed in order to adapt to the predicted changes.

The culmination of warmer and drier bioclimatic conditions by 2100 is depicted for Greece with the introduction of the dry conditions’ limited distribution for both investigated RCPs, where slightly more extended areas are expected to be impacted under the extreme RCP8.5 scenario.

The bioclimatic evolution towards warmer and drier conditions will compel the achievement of appropriate irrigation schedules to meet the future excessive water requirements of crops. This is especially true for the agricultural areas dominated by the semidry regime, which will depend on irrigation, and those characterized by Mediterranean conditions that will need supplementary irrigation. These tactics are hopefully expected to be implemented for the insurance of agricultural sustainability in most of the examined countries (Bulgaria, Greece, N. Macedonia, Romania and Serbia) projected to be climatically pressurized.

Finally, the present study's outcomes highlight the de Martonne index's usefulness for the depiction of southern Europe's bioclimate dryness levels for the territory's future natural and agricultural areas. Moreover, the thematic mapping and representations presented could be a useful tool in raising awareness and of importance to the informed citizen and decision-maker in drafting future strategies and planning, especially in protected areas.

At this point, we should note that the de Martonne index is annual, so it cannot identify possible changes in its intra-annual fluctuation. However, it remains extremely useful because it has already been used in many studies concerning ecology and agricultural production and is an index that requires easy-to-obtain data.

Future research should focus on examining the potential land use/landcover alterations regarding the bioclimatic change in the area, along with the impact on the related emissions and sustainability goals. Moreover, future studies could focus on the bioclimate's evolution over agricultural, natural and urban areas of central Europe by implementing ultrahigh-resolution computations of the de Martonne bioclimatic index and other appropriate bioclimatic indices.

**Supplementary Materials:** The following supporting information can be downloaded at: <https://www.mdpi.com/article/10.3390/atmos14050858/s1>, Figure S1: The dry IDM class during p3 in the RCP7 scenario; Figure S2: The dry IDM class during p3 under in RCP8.5 scenario.

**Author Contributions:** Conceptualization, I.C.; Methodology, I.C.; Investigation, F.D. and I.C.; Resources, F.D.; Original Preparation and Writing, F.D.; Writing on Data and Methods, I.C.; Method Application and Computation of Results, I.C.; Table and Figures, I.C.; Review and Editing, F.D.; Review and Editing overview, I.X.T. All authors have read and agreed to the published version of the manuscript.

**Funding:** This research received no external funding.

**Institutional Review Board Statement:** Not applicable.

**Informed Consent Statement:** Not applicable.

**Data Availability Statement:** The maps presented in this study are available in higher resolution upon request.

**Acknowledgments:** The authors would like to thank Jeffrey S. Evans for the very useful clarifications regarding the usage of the spatialEco package application.

**Conflicts of Interest:** The authors declare no conflict of interest.

## References

1. Charalampopoulos, I.; Droulia, F. The Agro-Meteorological Caused Famines as an Evolutionary Factor in the Formation of Civilisation and History: Representative Cases in Europe. *Climate* **2021**, *9*, 5. [CrossRef]
2. Bussotti, F.; Pollastrini, M. Traditional and Novel Indicators of Climate Change Impacts on European Forest Trees. *Forests* **2017**, *8*, 137. [CrossRef]
3. Bandoc, G.; Prăvălie, R.; Patriche, C.; Dragomir, E.; Tomescu, M. Response of Phenological Events to Climate Warming in the Southern and South-Eastern Regions of Romania. *Stoch. Environ. Res. Risk Assess.* **2018**, *32*, 1113–1129. [CrossRef]
4. Charalampopoulos, I.; Droulia, F.; Evans, J. The Bioclimatic Change of the Agricultural and Natural Areas of the Adriatic Coastal Countries. *Sustainability* **2023**, *15*, 4867. [CrossRef]
5. Kokkoris, I.P.; Bekri, E.S.; Skuras, D.; Vlami, V.; Zogaris, S.; Maroulis, G.; Dimopoulos, D.; Dimopoulos, P. Integrating MAES Implementation into Protected Area Management under Climate Change: A Fine-Scale Application in Greece. *Sci. Total Environ.* **2019**, *695*, 133530. [CrossRef]
6. Kokkoris, I.P.; Skuras, D.; Maniatis, Y.; Dimopoulos, P. Natura 2000 Public Awareness in EU: A Prerequisite for Successful Conservation Policy. *Land Use Policy* **2023**, *125*, 106482. [CrossRef]
7. Droulia, F.; Charalampopoulos, I. Future Climate Change Impacts on European Viticulture: A Review on Recent Scientific Advances. *Atmosphere* **2021**, *12*, 495. [CrossRef]
8. Nistor, M.-M. Climate Change Effect on Groundwater Resources in South East Europe during 21st Century. *Quat. Int.* **2019**, *504*, 171–180. [CrossRef]
9. Perera, A.T.D.; Nik, V.M.; Chen, D.; Scartezini, J.-L.; Hong, T. Quantifying the Impacts of Climate Change and Extreme Climate Events on Energy Systems. *Nat. Energy* **2020**, *5*, 150–159. [CrossRef]

10. Alimonti, G.; Mariani, L.; Prodi, F.; Ricci, R.A. A Critical Assessment of Extreme Events Trends in Times of Global Warming. *Eur. Phys. J. Plus* **2022**, *137*, 112. [[CrossRef](#)]
11. Charalampopoulos, I. Agrometeorological Conditions and Agroclimatic Trends for the Maize and Wheat Crops in the Balkan Region. *Atmosphere* **2021**, *12*, 671. [[CrossRef](#)]
12. Giannakopoulos, C.; Kostopoulou, E.; Varotsos, K.V.; Tziotziou, K.; Plitharas, A. An Integrated Assessment of Climate Change Impacts for Greece in the near Future. *Reg. Environ. Change* **2011**, *11*, 829–843. [[CrossRef](#)]
13. Cheval, S.; Dumitrescu, A.; Birsan, M.-V. Variability of the Aridity in the South-Eastern Europe over 1961–2050. *CATENA* **2017**, *151*, 74–86. [[CrossRef](#)]
14. Pravalie, R.; Sîrodoev, I.; Peptenatu, D. Detecting Climate Change Effects on Forest Ecosystems in Southwestern Romania Using Landsat TM NDVI Data. *J. Geogr. Sci.* **2014**, *24*, 815–832. [[CrossRef](#)]
15. Georgieva, V.; Kazandjiev, V.; Bozhanova, V.; Mihova, G.; Ivanova, D.; Todorovska, E.; Uhr, Z.; Ilchovska, M.; Sotirov, D.; Malasheva, P. Climatic Changes—A Challenge for the Bulgarian Farmers. *Agriculture* **2022**, *12*, 2090. [[CrossRef](#)]
16. Tošić, I.; Unkašević, M.; Putniković, S. Extreme Daily Precipitation: The Case of Serbia in 2014. *Theor. Appl. Clim.* **2017**, *128*, 785–794. [[CrossRef](#)]
17. Mavrakis, A.; Salvati, L. Analyzing the Behaviour of Selected Risk Indexes during the 2007 Greek Forest Fires. *Int. J. Environ. Res.* **2015**, *9*, 831–840.
18. Ciceu, A.; Popa, I.; Leca, S.; Pitar, D.; Chivulescu, S.; Badea, O. Climate Change Effects on Tree Growth from Romanian Forest Monitoring Level II Plots. *Sci. Total Environ.* **2020**, *698*, 134129. [[CrossRef](#)]
19. Češljár, G.; Jovanović, F.; Brašanac-Bosanac, L.; Đorđević, I.; Mitrović, S.; Eremija, S.; Ćirković-Mitrović, T.; Lučić, A. Impact of an Extremely Dry Period on Tree Defoliation and Tree Mortality in Serbia. *Plants* **2022**, *11*, 1286. [[CrossRef](#)]
20. Sidor, C.G.; Camarero, J.J.; Popa, I.; Badea, O.; Apostol, E.N.; Vlad, R. Forest Vulnerability to Extreme Climatic Events in Romanian Scots Pine Forests. *Sci. Total Environ.* **2019**, *678*, 721–727. [[CrossRef](#)]
21. Avram, S.; Ontel, I.; Gheorghe, C.; Rodino, S.; Roșca, S. Applying a Complex Integrated Method for Mapping and Assessment of the Degraded Ecosystem Hotspots from Romania. *Int. J. Environ. Res. Public Health* **2021**, *18*, 11416. [[CrossRef](#)]
22. Kougioumoutzis, K.; Kokkoris, I.P.; Panitsa, M.; Trigas, P.; Strid, A.; Dimopoulos, P. Spatial Phylogenetics, Biogeographical Patterns and Conservation Implications of the Endemic Flora of Crete (Aegean, Greece) under Climate Change Scenarios. *Biology* **2020**, *9*, 199. [[CrossRef](#)] [[PubMed](#)]
23. Jelena, T.-D.; Ivana, Z.; Dragana, S.; Mihailo, G. Climate Changes and Invasive Plant Species: Raising the Awareness of the Public towards Alien Invasive Plant Species in the City of Belgrade. *FEBS Fresenius Environ. Bull.* **2016**, *25*, 4680.
24. Iannella, M.; D’Alessandro, P.; Biondi, M. Forecasting the Spread Associated with Climate Change in Eastern Europe of the Invasive Asiatic Flea Beetle, *Luperomorpha Xanthodera* (Coleoptera: Chrysomelidae). *Eur. J. Entomol.* **2020**, *117*, 130–138. [[CrossRef](#)]
25. Gao, X.; Giorgi, F. Increased Aridity in the Mediterranean Region under Greenhouse Gas Forcing Estimated from High Resolution Simulations with a Regional Climate Model. *Glob. Planet. Change* **2008**, *62*, 195–209. [[CrossRef](#)]
26. Nistor, M.-M.; Dezsi, Ș.; Cheval, S.; Baciu, M. Climate Change Effects on Groundwater Resources: A New Assessment Method through Climate Indices and Effective Precipitation in Beliș District, Western Carpathians. *Meteorol. Appl.* **2016**, *23*, 554–561. [[CrossRef](#)]
27. Nistor, M.-M.; Ronchetti, F.; Corsini, A.; Cheval, S.; Dumitrescu, A.; Rai, P.K.; Petrea, D.; Dezsi, Ș. Crop Evapotranspiration Variation under Climate Change in South East Europe during 1991–2050. *Carpathian J. Earth Environ. Sci.* **2017**, *12*, 571–582.
28. Iizumi, T.; Ramankutty, N. Changes in Yield Variability of Major Crops for 1981–2010 Explained by Climate Change. *Environ. Res. Lett.* **2016**, *11*, 034003. [[CrossRef](#)]
29. Droulia, F.; Charalampopoulos, I. A Review on the Observed Climate Change in Europe and Its Impacts on Viticulture. *Atmosphere* **2022**, *13*, 837. [[CrossRef](#)]
30. Cardell, M.F.; Amengual, A.; Romero, R. Future Effects of Climate Change on the Suitability of Wine Grape Production across Europe. *Reg. Environ. Change* **2019**, *19*, 2299–2310. [[CrossRef](#)]
31. Ontel, I.; Vladut, A. Impact of Drought on the Productivity of Agricultural Crops within the Oltenia Plain, Romania. *Geogr. Pannonica* **2015**, *19*, 9–19. [[CrossRef](#)]
32. Charalampopoulos, I.; Droulia, F. Frost Conditions Due to Climate Change in South-Eastern Europe via a High-Spatiotemporal-Resolution Dataset. *Atmosphere* **2022**, *13*, 1407. [[CrossRef](#)]
33. Charalampopoulos, I.; Polychroni, I.; Psomiadis, E.; Nastos, P. Spatiotemporal Estimation of the Olive and Vine Cultivations’ Growing Degree Days in the Balkans Region. *Atmosphere* **2021**, *12*, 148. [[CrossRef](#)]
34. Baltas, E. Spatial distribution of climatic indices in northern Greece. *Meteorol. Appl.* **2007**, *14*, 69–78. [[CrossRef](#)]
35. Savo, V.; Zuliani, E.; Salvati, L.; Perini, L.; Caneva, G. Long-Term Changes in Precipitation and Temperature Patterns and Their Possible Impacts on Vegetation (Tolfa-Cerite Area, Central Italy). *Appl. Ecol. Environ. Res.* **2012**, *10*, 243–266. [[CrossRef](#)]
36. Lazoglou, G.; Anagnostopoulou, C.; Koundouras, S. Climate Change Projections for Greek Viticulture as Simulated by a Regional Climate Model. *Theor. Appl. Climatol.* **2018**, *133*, 551–567. [[CrossRef](#)]
37. Charalampopoulos, I.; Tsiros, I.; Chronopoulou-Sereli, A.; Matzarakis, A. Analysis of Thermal Bioclimate in Various Urban Configurations in Athens, Greece. *Urban Ecosyst.* **2013**, *16*, 217–233. [[CrossRef](#)]

38. Founda, D.; Katavoutas, G.; Pierros, F.; Mihalopoulos, N. Centennial Changes in Heat Waves Characteristics in Athens (Greece) from Multiple Definitions Based on Climatic and Bioclimatic Indices. *Glob. Planet. Change* **2022**, *212*, 103807. [[CrossRef](#)]
39. Mihăilă, D.; Bistricean, P.-I.; Briciu, A.-E. Assessment of the Climate Potential for Tourism. Case Study: The North-East Development Region of Romania. *Theor. Appl. Clim.* **2019**, *137*, 601–622. [[CrossRef](#)]
40. Bhuyan, U.; Zang, C.; Menzel, A. Different Responses of Multispecies Tree Ring Growth to Various Drought Indices across Europe. *Dendrochronologia* **2017**, *44*, 1–8. [[CrossRef](#)]
41. Ugarković, D.; Paulić, V.; Šapić, I.; Poljak, I.; Ančić, M.; Tikvić, I.; Stankić, I. Climatic Relationship of Vegetation in Forest Stands in the Mediterranean Vegetation Belt of the Eastern Adriatic. *Atmosphere* **2022**, *13*, 1709. [[CrossRef](#)]
42. Haidu, I.; Nistor, M.-M. Long-Term Effect of Climate Change on Groundwater Recharge in the Grand Est Region of France. *Meteorol. Appl.* **2020**, *27*, e1796. [[CrossRef](#)]
43. Emadodin, I.; Corral, D.E.F.; Reinsch, T.; Kluß, C.; Taube, F. Climate Change Effects on Temperate Grassland and Its Implication for Forage Production: A Case Study from Northern Germany. *Agriculture* **2021**, *11*, 232. [[CrossRef](#)]
44. Baltas, E.A. Climatic Conditions and Availability of Water Resources in Greece. *Int. J. Water Resour. Dev.* **2008**, *24*, 635–649. [[CrossRef](#)]
45. Mavrakis, A.; Colantoni, A.; Salvati, L. Soil Degradation, Landscape and Climate Variations in a Mediterranean Agro-Forest System (Thriasio, Greece): Proposal for a Desertification Indicator Using Time Series Analysis. *Int. J. Agric. Resour. Gov. Ecol.* **2014**, *10*, 335–343. [[CrossRef](#)]
46. Beloiu, M.; Poursanidis, D.; Tsakirakis, A.; Chrysoulakis, N.; Hoffmann, S.; Lymberakis, P.; Barnias, A.; Kienle, D.; Beierkuhnlein, C. No Treeline Shift despite Climate Change over the Last 70 Years. *For. Ecosyst.* **2022**, *9*, 100002. [[CrossRef](#)]
47. Sidiropoulou, A.; Chouvardas, D.; Mantzanas, K.; Stefanidis, S.; Karatassiou, M. Impact of Transhumant Livestock Grazing Abandonment on Pseudo-Alpine Grasslands in Greece in the Context of Climatic Change. *Land* **2022**, *11*, 2126. [[CrossRef](#)]
48. Mattas, C.; Anagnostopoulou, C.; Venetsanou, P.; Bilas, G.; Lazoglou, G. Evaluation of Extreme Dry and Wet Conditions Using Climate and Hydrological Indices in the Upper Part of the Gallikos River Basin. *Proceedings* **2018**, *7*, 3. [[CrossRef](#)]
49. Lappas, I.; Zorapas, V.; Kaloumenos, K. Estimation and Surface Distribution of Climate Indices in the Water District of Central–Eastern Greece. In Proceedings of the 10th International Hydrogeological Congress of Greece, Thessaloniki, Greece, 8 October 2014.
50. Bačević, N.; Vukočić, D.; Nikolić, M.; Janc, N.; Milentijević, N.; Gavrilov, M. Aridity in Kosovo and Metohija, Serbia. *Carpathian J. Earth Environ. Sci.* **2017**, *12*, 563–570.
51. Hrnjak, I.; Lukić, T.; Gavrilov, M.B.; Marković, S.B.; Unkašević, M.; Tošić, I. Aridity in Vojvodina, Serbia. *Theor. Appl. Clim.* **2014**, *115*, 323–332. [[CrossRef](#)]
52. Gavrilov, M.B.; Radaković, M.G.; Sipos, G.; Mezösi, G.; Gavrilov, G.; Lukić, T.; Basarin, B.; Benyhe, B.; Fiala, K.; Kozák, P.; et al. Aridity in the Central and Southern Pannonian Basin. *Atmosphere* **2020**, *11*, 1269. [[CrossRef](#)]
53. Gavrilov, M.B.; An, W.; Xu, C.; Radaković, M.G.; Hao, Q.; Yang, F.; Guo, Z.; Perić, Z.; Gavrilov, G.; Marković, S.B. Independent Aridity and Drought Pieces of Evidence Based on Meteorological Data and Tree Ring Data in Southeast Banat, Vojvodina, Serbia. *Atmosphere* **2019**, *10*, 586. [[CrossRef](#)]
54. Radaković, M.G.; Tošić, I.; Bačević, N.; Mladjan, D.; Gavrilov, M.B.; Marković, S.B. The Analysis of Aridity in Central Serbia from 1949 to 2015. *Theor. Appl. Clim.* **2018**, *133*, 887–898. [[CrossRef](#)]
55. Moteva, M.; Kazandjiev, V.; Georgieva, V. Climate Change and the Hydrothermal and Evapotranspiration Conditions in the Planning Regions of Bulgaria. In Proceedings of the Fourteenth International Water Technology Conference—IWTC 2010, Cairo, Egypt, 21–23 March 2010.
56. Vlăduț, A.; Nikolova, N.; Licurici, M. Aridity Assessment within Southern Romania and Northern Bulgaria. *Hrvat. Geogr. Glas.* **2017**, *79*, 5–26. [[CrossRef](#)]
57. Raev, I.; Alexandrov, V.; Tinchev, G. Assessment of Drought Related Climate Change Impacts on Forests in Bulgaria. *Silva Balc.* **2015**, *16*, 5–24.
58. Strat, D. Trends in Climate and Bioclimate Profile of Sărăturile Beach Ridges Plain-Danube Delta. *Ovidius Univ. Ann.* **2010**, *5*, 17–30.
59. Paltineanu, C.; Tanasescu, N.; Chitu, E.; Mihailescu, I.F. Relationships between the De Martonne Aridity Index and Water Requirements of Some Representative Crops: A Case Study from Romania. *Int. Agrophys.* **2007**, *21*, 81–93.
60. Paltineanu, C.; Mihailescu, I.F.; Seceleanu, I.; Dragota, C.; Vasenciuc, F. Using Aridity Indices to Describe Some Climate and Soil Features in Eastern Europe: A Romanian Case Study. *Theor. Appl. Climatol.* **2007**, *90*, 263–274. [[CrossRef](#)]
61. Croitoru, A.-E.; Piticar, A.; Imbroane, A.M.; Burada, D.C. Spatiotemporal Distribution of Aridity Indices Based on Temperature and Precipitation in the Extra-Carpathian Regions of Romania. *Theor. Appl. Clim.* **2013**, *112*, 597–607. [[CrossRef](#)]
62. Vladut, A. Ecoclimatic Indexes within the Oltenia Plain. *Forum Geogr.* **2010**, *9*, 49–56.
63. Prăvălie, R. Climate Issues on Aridity Trends of Southern Oltenia in the Last Five Decades. *Geogr. Tech.* **2013**, *1*, 70–79.
64. Vlăduț, A.Ș.; Licurici, M. Aridity Conditions within the Region of Oltenia (Romania) from 1961 to 2015. *Theor. Appl. Clim.* **2020**, *140*, 589–602. [[CrossRef](#)]
65. Lungu, M.; Panaitescu, L.; Niță, S. Aridity, Climatic Risk Phenomenon in Dobruja. *Present Environ. Sustain. Dev.* **2011**, *5*, 179–190.
66. Prăvălie, R.; Bandoc, G. Aridity Variability in the Last Five Decades in the Dobrogea Region, Romania. *Arid Land Res. Manag.* **2015**, *29*, 265–287. [[CrossRef](#)]

67. Tiscovschi, A.; Manea, G.; Cocos, O.; Vijulie, I.; Cuculici, R. Characteristics of Aridity Conditions in Sout Dobroudja. *Riscuri Si Catastr. Casa Cărbii De Știință Cluj-Napoca XII* **2013**, *12*, 57–65.
68. Vorovencii, I. Applying the Change Vector Analysis Technique to Assess the Desertification Risk in the South-West of Romania in the Period 1984–2011. *Environ. Monit Assess* **2017**, *189*, 524. [[CrossRef](#)]
69. Pravalie, R.; Sirodoev, I.; Peptenatu, D. Changes in the Forest Ecosystems in Areas Impacted by Aridization in South-Western Romania. *J. Environ. Health Sci Eng.* **2014**, *12*, 2. [[CrossRef](#)]
70. Man, T.E.; Armas, A.; Beilicci, R.; Beilicci, E. Assessment Regarding the Evolution in Time (1980–2014) of Drought on the Basis of Several Computation Indexes: Study Case Timisoara. *Nat. Resour. Sustain. Dev.* **2018**, *8*, 1–8. [[CrossRef](#)]
71. Mihai, G.; Alexandru, A.-M.; Nita, I.-A.; Birsan, M.-V. Climate Change in the Provenance Regions of Romania over the Last 70 Years: Implications for Forest Management. *Forests* **2022**, *13*, 1203. [[CrossRef](#)]
72. Milovanović, B.; Schubert, S.; Radovanović, M.; Vakanjac, V.R.; Schneider, C. Projected Changes in Air Temperature, Precipitation and Aridity in Serbia in the 21st Century. *Int. J. Climatol.* **2022**, *42*, 1985–2003. [[CrossRef](#)]
73. Butchart, N.; Anstey, J.A.; Kawatani, Y.; Osprey, S.M.; Richter, J.H.; Wu, T. QBO Changes in CMIP6 Climate Projections. *Geophys. Res. Lett.* **2020**, *47*, e2019GL086903. [[CrossRef](#)]
74. Ceglar, A.; Toreti, A.; Zampieri, M.; Royo, C. Global Loss of Climatically Suitable Areas for Durum Wheat Growth in the Future. *Environ. Res. Lett.* **2021**, *16*, 104049. [[CrossRef](#)]
75. Kolanowska, M.; Michalska, E.; Konowalik, K. The Impact of Global Warming on the Niches and Pollinator Availability of Sexually Deceptive Orchid with a Single Pollen Vector. *Sci. Total Environ.* **2021**, *795*, 148850. [[CrossRef](#)] [[PubMed](#)]
76. Chemura, A.; Mudereri, B.T.; Yalew, A.W.; Gornott, C. Climate Change and Specialty Coffee Potential in Ethiopia. *Sci. Rep.* **2021**, *11*, 8097. [[CrossRef](#)] [[PubMed](#)]
77. Wang, W.; Zhu, Q.; He, G.; Liu, X.; Peng, W.; Cai, Y. Impacts of Climate Change on Pine Wilt Disease Outbreaks and Associated Carbon Stock Losses. *Agric. For. Meteorol.* **2023**, *334*, 109426. [[CrossRef](#)]
78. Reddy, N.M.; Saravanan, S. Extreme Precipitation Indices over India Using CMIP6: A Special Emphasis on the SSP585 Scenario. *Environ. Sci. Pollut. Res.* **2023**, *30*, 47119–47143. [[CrossRef](#)]
79. Tollefson, J. What the War in Ukraine Means for Energy, Climate and Food. *Nature* **2022**, *604*, 232–233. [[CrossRef](#)]
80. Dong, N.; You, L.; Cai, W.; Li, G.; Lin, H. Land Use Projections in China under Global Socioeconomic and Emission Scenarios: Utilizing a Scenario-Based Land-Use Change Assessment Framework. *Glob. Environ. Change* **2018**, *50*, 164–177. [[CrossRef](#)]
81. Yang, W.; Ma, Y.; Jing, L.; Wang, S.; Sun, Z.; Tang, Y.; Li, H. Differential Impacts of Climatic and Land Use Changes on Habitat Suitability and Protected Area Adequacy across the Asian Elephant’s Range. *Sustainability* **2022**, *14*, 4933. [[CrossRef](#)]
82. Donmez, C.; Schmidt, M.; Cilek, A.; Grosse, M.; Paul, C.; Hierold, W.; Helming, K. Climate Change Impacts on Long-Term Field Experiments in Germany. *Agric. Syst.* **2023**, *205*, 103578. [[CrossRef](#)]
83. Jägermeyr, J.; Müller, C.; Ruane, A.C.; Elliott, J.; Balkovic, J.; Castillo, O.; Faye, B.; Foster, I.; Folberth, C.; Franke, J.A.; et al. Climate Impacts on Global Agriculture Emerge Earlier in New Generation of Climate and Crop Models. *Nat. Food* **2021**, *2*, 873–885. [[CrossRef](#)] [[PubMed](#)]
84. Yao, L.; Zhou, H.; Yan, Y.; Su, Y. Projection of Suitability for the Typical Agro-Ecological Types in Central Asia under Four SSP-RCP Scenarios. *Eur. J. Agron.* **2022**, *140*, 126599. [[CrossRef](#)]
85. Karger, D.N.; Wilson, A.M.; Mahony, C.; Zimmermann, N.E.; Jetz, W. Global Daily 1 Km Land Surface Precipitation Based on Cloud Cover-Informed Downscaling. *Sci. Data* **2021**, *8*, 307. [[CrossRef](#)]
86. Karger, D.N.; Schmatz, D.R.; Dettling, G.; Zimmermann, N.E. High-Resolution Monthly Precipitation and Temperature Time Series from 2006 to 2100. *Sci. Data* **2020**, *7*, 248. [[CrossRef](#)]
87. Guo, F.; Lenoir, J.; Bonebrake, T.C. Land-Use Change Interacts with Climate to Determine Elevational Species Redistribution. *Nat. Commun.* **2018**, *9*, 1315. [[CrossRef](#)]
88. Margalef-Marrase, J.; Pérez-Navarro, M.Á.; Lloret, F. Relationship between Heatwave-Induced Forest Die-off and Climatic Suitability in Multiple Tree Species. *Glob. Change Biol.* **2020**, *26*, 3134–3146. [[CrossRef](#)] [[PubMed](#)]
89. Christia, C.; Giordani, G.; Papastergiadou, E. Environmental Variability and Macrophyte Assemblages in Coastal Lagoon Types of Western Greece (Mediterranean Sea). *Water* **2018**, *10*, 151. [[CrossRef](#)]
90. Lembrechts, J.J.; Lenoir, J.; Roth, N.; Hattab, T.; Milbau, A.; Haider, S.; Pellissier, L.; Pauchard, A.; Ratier Backes, A.; Dimarco, R.D.; et al. Comparing Temperature Data Sources for Use in Species Distribution Models: From in-Situ Logging to Remote Sensing. *Glob. Ecol. Biogeogr.* **2019**, *28*, 1578–1596. [[CrossRef](#)]
91. Evans, J.S.; Murphy, M.A.; Ram, K. SpatialEco: Spatial Analysis and Modelling Utilities. 2022. Available online: <https://CRAN.R-project.org/package=spatialEco> (accessed on 12 December 2022).
92. Wickham, H. The Tidyverse. Available online: <https://www.tidyverse.org/> (accessed on 15 December 2022).
93. Hijmans, R.J.; Bivand, R.; Forner, K.; Ooms, J.; Pebesma, E.; Sumner, M.D. Terra: Spatial Data Analysis. 2023. Available online: <https://CRAN.R-project.org/package=terra> (accessed on 7 July 2022).
94. Rogelj, J.; Popp, A.; Calvin, K.V.; Luderer, G.; Emmerling, J.; Gernaat, D.; Fujimori, S.; Strefler, J.; Hasegawa, T.; Marangoni, G.; et al. Scenarios towards Limiting Global Mean Temperature Increase below 1.5 °C. *Nat. Clim. Change* **2018**, *8*, 325–332. [[CrossRef](#)]
95. Meinshausen, M.; Nicholls, Z.R.J.; Lewis, J.; Gidden, M.J.; Vogel, E.; Freund, M.; Beyerle, U.; Gessner, C.; Nauels, A.; Bauer, N.; et al. The Shared Socio-Economic Pathway (SSP) Greenhouse Gas Concentrations and Their Extensions to 2500. *Geosci. Model Dev.* **2020**, *13*, 3571–3605. [[CrossRef](#)]

96. O'Neill, B.C.; Tebaldi, C.; van Vuuren, D.P.; Eyring, V.; Friedlingstein, P.; Hurtt, G.; Knutti, R.; Kriegler, E.; Lamarque, J.-F.; Lowe, J.; et al. The Scenario Model Intercomparison Project (ScenarioMIP) for CMIP6. *Geosci. Model Dev.* **2016**, *9*, 3461–3482. [[CrossRef](#)]
97. De Martonne, E. Regions of Interior-Basin Drainage. *Geogr. Rev.* **1927**, *17*, 397–414. [[CrossRef](#)]
98. Passarella, G.; Bruno, D.; Lay-Ekuakille, A.; Maggi, S.; Masciale, R.; Zaccaria, D. Spatial and Temporal Classification of Coastal Regions Using Bioclimatic Indices in a Mediterranean Environment. *Sci. Total Environ.* **2020**, *700*, 134415. [[CrossRef](#)] [[PubMed](#)]
99. European Environment Agency. CORINE Land Cover. Available online: <http://www.eea.europa.eu/publications/COR0-landcover> (accessed on 5 March 2017).
100. QGIS Development Team. *QGIS Geographic Information System*; QGIS Association: Grüt, Switzerland, 2009.
101. Tsiros, I.X.; Nastos, P.; Proutsos, N.D.; Tsaousidis, A. Variability of the Aridity Index and Related Drought Parameters in Greece Using Climatological Data over the Last Century (1900–1997). *Atmos. Res.* **2020**, *240*, 104914. [[CrossRef](#)]

**Disclaimer/Publisher's Note:** The statements, opinions and data contained in all publications are solely those of the individual author(s) and contributor(s) and not of MDPI and/or the editor(s). MDPI and/or the editor(s) disclaim responsibility for any injury to people or property resulting from any ideas, methods, instructions or products referred to in the content.